

The hydrogen molecule in magnetic fields: The ground states of the Σ manifold of the parallel configuration

T. Detmer, P. Schmelcher, F. K. Diakonov and L. S. Cederbaum
*Theoretische Chemie, Physikalisch-Chemisches Institut,
 Universität Heidelberg, INF 253, D-69120 Heidelberg,
 Federal Republic of Germany*

The electronic structure of the hydrogen molecule is investigated for the parallel configuration. The ground states of the Σ manifold are studied for ungerade and gerade parity as well as singlet and triplet states covering a broad regime of field strengths from $B = 0$ up to $B = 100$ a.u.. A variety of interesting phenomena can be observed. For the $^1\Sigma_g$ state we found a monotonous decrease of the equilibrium distance and a simultaneously increase of the dissociation energy with growing magnetic-field strength. The $^3\Sigma_g$ state is shown to develop an additional minimum which has no counterpart in field-free space. The $^1\Sigma_u$ state shows a monotonous increase in the dissociation energy with first increasing and then decreasing internuclear distance of the minimum. For this state the dissociation channel is $H_2 \rightarrow H^- + H^+$ for magnetic-field strengths $B \gtrsim 20$ a.u. due to the existence of strongly bound H^- states in strong magnetic fields. The repulsive $^3\Sigma_u$ state possesses a very shallow van der Waals minimum for magnetic-field strengths smaller than 1.0 a.u. within the numerical accuracy of our calculations. The $^1\Sigma_g$ and $^3\Sigma_u$ states cross as a function of B and the $^3\Sigma_u$ state, which is an unbound state, becomes the ground state of the hydrogen molecule in magnetic fields $B \gtrsim 0.2$ a.u.. This is of particular interest for the existence of molecular hydrogen in the vicinity of white dwarfs. In superstrong fields the ground state is again a strongly bound state, the $^3\Pi_u$ state.

I. INTRODUCTION

During the past years the behavior and properties of particle systems in strong magnetic fields became a subject of increasing interest in different areas of physics like astrophysics or solid-state physics. In astrophysics the discovery of strong magnetic fields in the vicinity of white dwarfs ($B \lesssim 10^5 T$) and neutron stars ($B \lesssim 10^8 T$) [1–3] gave rise to many investigations. On the other hand, for highly excited atomic states the Coulomb forces and magnetic forces are of comparable orders of magnitude even for laboratory field strengths. In solid-state physics, excitons show strong field effects due to their small effective masses and large dielectricity constants [4].

A number of investigations were performed to reveal the structure and properties of small atoms and one-dimensional chains in such strong fields. They include variational methods [5–7], Thomas-Fermi-type models [8–11], density-functional calculations [12, 13] and Hartree-Fock calculations [14–18]. For a summary of energies, wave functions, and electromagnetic transitions concerning the hydrogen atom in strong magnetic fields, we refer the reader to Ref. [19].

In contrast to the large number of studies on in particular the hydrogen atom in a strong magnetic fields there exist only a few investigations on molecular systems. Most of them deal with the H_2^+ ion (see Refs. [20–26] and references therein) and little is known about the H_2 molecule [18, 27–31]. In strong magnetic fields we encounter a variety of interesting new molecular phenomena. For the ground state of the H_2^+ ion an increase of the electron density between the nuclear charges leads to a contraction of the bond length. At the same time we observe an increase in the dissociation energy with increasing magnetic-field strength. Moreover for the H_2^+ ion a class of states with purely repulsive potential energy curves (PECs) in field-free space was shown to exhibit well-pronounced potential-energy minima in a sufficiently strong magnetic field [21, 23]. Furthermore the topology of the electronic potential surfaces changes strongly with varying field strength. For intermediate field strengths it was shown, that the lowest-lying electronic states possess their global equilibrium configurations at positions corresponding to high symmetry, i.e., $\theta = 0^\circ$ or $\theta = 90^\circ$. However, for some excited states a global symmetry lowering occurs leading to global equilibrium configurations at $0^\circ < \theta < 90^\circ$ [24–26].

Only little is known concerning the electronic structure of the hydrogen molecule in a strong magnetic field. Most of the investigations deal with the hydrogen molecule in superstrong fields ($B \geq 10^{11} G$). For intermediate field strengths there exist only two studies of qualitative character which investigate the PEC of the lowest $^1\Sigma_g$ state [27, 28]. A detailed knowledge of the electronic structure of the hydrogen molecule is of particular relevance in astrophysics since it might lead to a better understanding of the spectra of white dwarfs and neutron stars. Hereby the ground state of the hydrogen molecule is of particular interest. Recently a controversial discussion arose concerning the electronic

structure of a hydrogen molecule in a superstrong magnetic field [30, 32–37]. It was conjectured that in superstrong magnetic fields the $^3\Sigma_u$ state would be the ground state of H_2 [32]. This state possesses a very shallow van der Waals minimum in field-free space at $R \sim 8 a.u.$. Due to the spin-Zeeman shift the $^3\Sigma_u$ state monotonously decreases in energy with increasing magnetic-field strength. Therefore a crossing exists between the $^1\Sigma_g$ and the $^3\Sigma_u$ state at some magnetic-field strength B_c . For that reason the authors expected the weakly bound $^3\Sigma_u$ state to be the ground state of the hydrogen molecule in superstrong fields. For such magnetic-field strengths, hydrogen might then be able to form a Bose-Einstein condensate and become superfluid. However it has been proved that the $^3\Pi_u$ state is the true ground state for magnetic-field strengths $B \gtrsim 3 \times 10^3 a.u.$ [30]. For magnetic-field strengths smaller than $B = 3 \times 10^3 a.u.$ the ground state of the hydrogen molecule is not known.

From the above it is evident that accurate investigations of the electronic structure of the hydrogen molecule are very desirable. In the present investigation we perform a first step to elucidate the electronic properties of the hydrogen molecule in a strong magnetic-field. Particular emphasis is placed on the intermediate regime which is of relevance to the physics of white dwarfs. We investigate the electronic structure of the lowest states of the Σ manifold, i.e., the lowest singlet and triplet states with gerade and ungerade parity for a magnetic quantum number equal to zero. We hereby focus on the case of the parallel internuclear and magnetic-field axes. This configuration is distinct by its higher symmetry compared to the case of an arbitrary angle θ between the internuclear and magnetic-field axis. It has been shown [38] that the diabatic energy curves exhibit extrema at $\theta = 0^\circ$, and it can therefore be expected that the parallel configuration plays an important role.

Our calculations will provide detailed data of equilibrium distances, total energies, and dissociation energies for the corresponding electronic states. Due to the efficiency of our method we are able to investigate the electronic structure in the complete range of field strengths, from $B = 0$ up to $B = 100 a.u.$

In detail the paper is organized as follows. In Sec. II we develop the theoretical framework as well as technical background for our calculations. Section III. is the central part of the paper. It contains the detailed discussion of the electronic PECs for the lowest $^1\Sigma_g$, $^1\Sigma_u$, $^3\Sigma_g$ and $^3\Sigma_u$ states for magnetic fields $B = 0 - 100 a.u.$. The summary and conclusions are given in Sec. IV. We use a basis set of nonspherical atomic orbitals for our configuration-interaction calculations [39]. Some details of this basis set are given in Appendix A. Furthermore, in Appendix A we describe the construction of the molecular wave function for the hydrogen molecule. Appendix B contains a more detailed description of the computational techniques. The evaluation of the matrix elements and some special features of the implementation of our source code are discussed to some extent.

II. THEORETICAL ASPECTS

We start with the total nonrelativistic molecular Hamiltonian in Cartesian coordinates. It is well known that the total pseudomomentum is a constant of motion [40, 41]. For a neutral system like the hydrogen molecule, the components of the pseudomomentum additionally commute with each other. Therefore, the Hamiltonian can be simplified by performing a so-called pseudoseparation of the center-of-mass motion [40, 42, 43]. Due to this pseudoseparation the center-of-mass coordinate and the conserved pseudomomentum are introduced as a pair of canonical conjugated variables. As a result, the center-of-mass coordinate does not appear in the transformed Hamiltonian. After applying this transformation, the exact Hamiltonian can be further simplified by a series of unitary transformations. For details of these transformations, we refer the reader to the literature [42, 43].

In order to separate the electronic and nuclear motion an adiabatic approximation has to be performed, which means that we have to apply the Born-Oppenheimer approximation in the presence of a magnetic field. The validity of the Born-Oppenheimer approximation in the presence of a magnetic field has been studied in detail by Schmelcher and coworkers [42–44], including all corrections due to finite nuclear mass. In a first order approximation we choose the electronic Hamiltonian as the fixed nuclei Hamiltonian, i.e., we assume infinitely heavy masses for the nuclei. The origin of our coordinate system coincides with the midpoint of the internuclear axis of the hydrogen molecule and the protons are located on the z axis. The magnetic field is chosen parallel to the z axis of our coordinate system and we use the symmetric gauge for the vector potential. Finally our electronic Hamiltonian takes on the following appearance:

$$H = \sum_{i=1}^2 \left\{ \frac{1}{2} \mathbf{p}_i^2 + \frac{1}{8} (\mathbf{B} \times \mathbf{r}_i)^2 + \frac{1}{2} \mathbf{L}_i \cdot \mathbf{B} - \frac{1}{|\mathbf{r}_i - \mathbf{R}/2|} - \frac{1}{|\mathbf{r}_i + \mathbf{R}/2|} \right\} + \frac{1}{|\mathbf{r}_1 - \mathbf{r}_2|} + \frac{1}{R} + \mathbf{S} \cdot \mathbf{B} \quad (1)$$

We hereby neglect relativistic effects such as, e.g., the spin-orbit coupling, and the gyromagnetic factor of the electron was chosen to be 2. The symbols \mathbf{r}_i , \mathbf{p}_i , and \mathbf{L}_i denote the position vectors, the canonical conjugated momenta and the angular momenta of the two electrons, respectively. \mathbf{B} and \mathbf{R} are the vectors of the magnetic field and internuclear

distance, respectively and R denotes the magnitude of \mathbf{R} . With \mathbf{S} we denote the vector of the total electronic spin. Since we deal with Σ states, the sum $\sum_{i=1}^2 \mathbf{L}_i \cdot \mathbf{B}$ equals to zero. Throughout the paper we will use atomic units.

The Hamiltonian (1) commutes with the following operators:

- a) The parity operator P due to the charge symmetry of the molecule. The corresponding eigenfunctions are marked with the subscript g for gerade or u for ungerade parity.
- b) The projection L_z of the electronic angular momentum on the internuclear axis.
- c) The square S^2 of the total electronic spin. The electronic functions are labeled with a left superscript describing the multiplicity $2S + 1$ of the state.
- d) The projection S_z of the total electronic spin on the internuclear axis. For singlet states the only possibility is $M_s = 0$. For triplet states we are only interested in the lowest state, which means $M_s = -1$.

In the absence of a magnetic field we encounter an additional symmetry namely the reflections with respect to the electronic coordinates at the xz (σ_v) plane. The eigenfunctions possess the corresponding eigenvalues ± 1 . This symmetry does not hold in the presence of a magnetic field. Therefore, the resulting symmetry groups for the hydrogen molecule are $D_{\infty h}$ in the case of field-free space, and $C_{\infty h}$ in the presence of a magnetic field [38].

In order to solve the fixed-nuclei electronic Schrödinger equation belonging to the Hamiltonian (1), we expand the electronic eigenfunctions in terms of molecular configurations. First of all we note that the total electronic wave function Ψ_{ges} can be written as a product of its spatial part Ψ and its spin part χ , i.e., we have $\Psi_{ges} = \Psi\chi$. For the spatial part Ψ of the wave function we use the linear combination of atomic orbitals molecular orbital ansatz (LCAO-MO), i.e., we decompose Ψ with respect to molecular orbital configurations ψ of H_2 which respect the corresponding symmetries (see above) and the Pauli principle, i.e

$$\begin{aligned} \Psi &= \sum_{i,j} c_{ij} [\psi_{ij}(\mathbf{r}_1, \mathbf{r}_2) \pm \psi_{ij}(\mathbf{r}_2, \mathbf{r}_1)] \\ &= \sum_{i,j} c_{ij} [\Phi_i(\mathbf{r}_1) \Phi_j(\mathbf{r}_2) \pm \Phi_i(\mathbf{r}_2) \Phi_j(\mathbf{r}_1)] \end{aligned}$$

The molecular-orbital configurations ψ_{ij} of H_2 are products of the corresponding one-electron H_2^+ molecular orbitals Φ_i and Φ_j . The H_2^+ molecular orbitals are built from atomic orbitals centered at each nucleus. A key ingredient of this procedure is a basis set of nonorthogonal optimized nonspherical Gaussian atomic orbitals which has been established previously [22, 39]. A more detailed description of the construction of the molecular electronic wave function is presented in Appendix A. In order to determine the molecular electronic wave function of H_2 we use the variation principle. This means we minimize the variational integral $\frac{\int \Psi^* H \Psi}{\int \Psi^* \Psi}$ by varying the coefficients c_i . The resulting generalized eigenvalue problem reads as follows:

$$(\underline{H} - \epsilon \underline{S}) \mathbf{c} = \mathbf{0} \quad (2)$$

In the present investigation for parallel internuclear axis and magnetic-field axis, the Hamiltonian matrix \underline{H} is real and symmetric and the overlap matrix is real, symmetric and positiv definite. The vector \mathbf{c} contains the expansion coefficients. The matrix elements of the Hamiltonian matrix and the overlap matrix are certain linear combinations of matrix elements with respect to the optimized nonspherical Gaussian atomic orbitals. The latter matrix elements were already calculated in Ref. [39]. However, the formulas for the electron-nucleus and in particular the electron-electron matrix elements given in Ref. [39] turned out to be not sufficiently efficient for numerical calculations with large basis sets. Both, the numerical stability and the efficient and fast computation of the matrix elements required a different approach to the integral evaluation within our basis set of atomic orbitals. In our computational scheme the matrix elements are evaluated by a combination of a special quadrature method and a subsequent numerical integration. We herefore wrote a numerical integration routine which is very carefully adjusted to the special problem of the hydrogen molecule parallel to a magnetic field. We were able to reduce the mean time of one integral calculation by a factor of 1000. Appendix B deals with the most important aspects of the corresponding computational method. For the construction of the Hamilton matrix within each subspace we used a direct method which means that each integral is evaluated only once. This procedure is very useful since the same atomic orbitals contribute to different molecular orbitals. In addition, all four matrices belonging to different subspaces (parity, spin multiplicity) of the Σ states are simultaneously constructed since they depend on the same matrix elements of the corresponding atomic orbitals.

For each PEC about 300 points were calculated on an average. In the present calculations, the typical dimension of the Hamiltonian matrix for each subspace varies between approximately 800 and 3000 depending on the magnetic-field strength. Depending on the dimension of the Hamiltonian matrix, it takes between 30 and 250 minutes for simultaneously calculating one point of a PEC of each Σ - subspace on a AIX 590 computer. Therefore, the total

amount of CPU time for our calculations amounts to approximately seven months on the above computer. Previous to the calculation of the PECs we performed detailed test on the accuracy and convergence of the calculations. For each magnetic-field strength we developed a basis set of atomic orbitals particularly adapted for minimizing the total energy. The overall accuracy of our results is estimated to be better than 10^{-3} . For the numerical solution of the eigenvalue problem (2) we used the standard NAG library.

III. RESULTS AND DISCUSSION

A. The $^1\Sigma_g$ state

Let us begin our investigation by considering the lowest $^1\Sigma_g$ state of the hydrogen molecule, which is the ground state in field-free space. This state has been extensively studied in field-free space in the adiabatic approximation, both theoretically and experimentally. For the literature on theoretical investigations up to 1960 we refer the reader to the bibliography in Ref. [45]. In particular we mention the pioneering work of James and Coolidge [46]. They represent the wave function in elliptic coordinates and demonstrated the usefulness of explicitly including the interelectronic distance in the wave function. A well-known drawback of the expansion in elliptical coordinates is that it converges more and more slowly with increasing values of the internuclear distance. In addition, the results of earlier work do not possess the accuracy needed for comparison with experimental data. Recently, several theoretical investigations were performed to improve the overall energy values for the $^1\Sigma_g^+$ state. Kolos [47] as well as Wolniewicz [48] improved the electronic energy calculated in the Born-Oppenheimer approximation several times. As a reference in the case of field-free space, we use the energy values obtained by Wolniewicz in 1995 [48].

In field-free space the energy curve of the $^1\Sigma_g^+$ state shows only one minimum at the equilibrium distance of 1.4 a.u. with a total energy of -1.1744757 a.u. . In the dissociation limit we have two H atoms in their ground states, i.e., $H_2 \rightarrow H(1s) + H(1s)$. Therefore, in the separated atom limit the total energy approaches -1.0 a.u. which corresponds to the energy of two H atoms in the ground state. In the united atom limit we have a helium atom in the $^1S 1s^2$ state. For that reason the total energy without the nucleus-nucleus repulsion $\frac{1}{R}$ approaches an energy value of 2.90372 a.u. with decreasing internuclear distance which is the ground state energy of the helium atom.

For the total energy at the equilibrium distance in field-free space we obtained a total energy of -1.173892 a.u. which yields a dissociation energy of 0.173892 a.u. . This corresponds to a relative accuracy in the total energy of about 6×10^{-4} compared to the benchmark result in Ref. [48]. This accuracy in the total energy even increases with increasing internuclear distance. For $R = 3 \text{ a.u.}$ and $R = 4 \text{ a.u.}$ we yield an error of 3×10^{-4} and 2×10^{-4} , respectively.

Let us explain how we obtained such an accuracy for a configuration-interaction (CI) calculation with a nonspherical Gaussian basis set. In order to compare the efficiency of our basis set with the best data available in the literature [48], we performed a calculation at the equilibrium distance for the ground state of H_2 . In this calculation we include 42 atomic basis functions constituting the H_2^+ orbitals with a magnetic quantum number equal to zero, 21 with gerade and 21 with ungerade parity, respectively. Hereby 24 atomic basis functions were optimized in order to describe the ground state of the hydrogen atom. In order to describe the in-out correlation correctly, 18 further atomic basis functions were optimized for excited states of the hydrogen atom. The in-out correlation takes into account the fact that if one electron is located near the internuclear axis, the second electron is preferably located far from the internuclear axis. The angular correlation describing the fact that the angle between the two electrons preferably differs by 180 degrees has been taken into account by using the following atomic basis functions: 32 functions for each of the magnetic quantum numbers $m = +1$ and $m = -1$; 18 functions for $m = +2$ and $m = -2$; and analogously 12 functions with $m = +3$ and $m = -3$. In order to understand the origin of the small difference of our dissociation energy compared to the dissociation energy given in Ref. [48] we performed an additional calculation and included only the 42 functions described above with magnetic quantum number equal to zero. This yields the so-called σ limit [49] of 1.1615 a.u. which is the lowest energy achievable by molecular configurations including only functions with a magnetic quantum number equal to zero. Our calculation yields 1.16144 a.u. for the σ limit. Therefore the main difference between the benchmark energy for the ground state of the H_2 molecule and our energy is due to some missing in-out correlation and angular correlation.

For the calculation of the entire PEC we used a second slightly smaller basis set than the one given above. The evaluation of the matrix elements takes increasingly more CPU time if higher angular momenta are involved. For the calculation of the PEC we therefore reduced the number of basis functions involving higher angular momenta in the following way: nine functions for each of the magnetic quantum numbers $m = +1$ and $m = -1$, and six functions for $m = +2$ and $m = -2$ were used. This reduction of our basis leads to only minor changes in the total energy but saves about 30 % of the CPU time needed for the evaluation of the matrix elements. In Table I both results for the

ground state energy of the hydrogen molecule are included. The calculations with respect to other electronic states of the hydrogen molecule in field-free space were performed by using the second basis set described above. Details of the basis set can be obtained from the authors upon request.

In contrast to the numerous investigations concerning the behavior and structure of the hydrogen molecule in field-free space only a few studies deal with the hydrogen molecule in strong magnetic fields [18, 27–32, 50]. Most of these deal with the hydrogen molecule in superstrong magnetic fields as large 10^{11} or even 10^{12} G (in atomic units this corresponds to $B = 42.54414$ a.u. and $B = 425.4414$ a.u., respectively).

First of all we mention that our computational method is by no means restricted to a special range of the magnetic-field strength. We were therefore able to study the development of the total energy with respect to the field strength ranging from field-free space up to a very strong field. Before entering into a discussion of our results let us introduce our notation for the united and separated atom limit in the presence of a magnetic field. Throughout this paper we will denote the atomic hydrogen states in the dissociation limit with $H(m_a^{\pi_a})$, where m_a denotes the atomic magnetic quantum number and π_a the atomic z parity, respectively. The united atom limit is described by $^{2S+1}L_z^{\pi_z}$. Here $2S+1$ is the spin multiplicity, L_z is the projection of the electronic angular momentum onto the axis of the magnetic field and π_z is the z parity. Now we are in the position to discuss the structure of the electronic PEC for the $^1\Sigma_g$ state in the presence of a magnetic field.

Figure 1 shows the energy curves of the $^1\Sigma_g$ state of the hydrogen molecule for different field strengths. In order to display electronic energies for varying magnetic-field strengths in the same viewgraph the energy in the dissociation limit is subtracted from the total energy, i.e., we show the quantity $E(R) = E_t(R) - \lim_{R \rightarrow \infty} E_t(R)$. The total as well as the dissociation energies at the equilibrium distance of the $^1\Sigma_g$ state are given in Table I together with the corresponding equilibrium internuclear distance for field strengths in the range $B = 0 - 100$ a.u.. Furthermore, we show the total energy in the dissociation limit, i.e., $\lim_{R \rightarrow \infty} E_t(R)$. For the $^1\Sigma_g$ state the dissociation channel is $H_2 \rightarrow H(0^+) + H(0^+)$ which means that the energy in the dissociation limit corresponds to the energy of two hydrogen atoms in the lowest electronic state with positive z parity. The appropriate electronic state in the united atom limit is the $^10^+$ helium state for any field strengths up to $B = 100$ a.u..

In the following we discuss the changes in the dissociation energy and equilibrium distance with increasing strength of the magnetic field. The overall behavior we observe in Table I is a monotonously increasing total energy as well as dissociation energy and a monotonously decreasing equilibrium internuclear distance. The decrease in the equilibrium internuclear distance originates from the simultaneous decrease of the electron clouds perpendicular and parallel to the magnetic field. Figure 1 illustrates the drastic growth in the dissociation energy for magnetic-field strengths $B \lesssim 1$ a.u.. At the same time the potential well becomes more and more pronounced, i.e., its width decreases strongly. Furthermore, the asymptotic behavior of the PEC for large values of R changes with the magnetic-field strength. With an increasing value of B the dissociation limit is reached at much smaller values of the internuclear distance, i.e. the onset of the asymptotic behavior can be observed for much smaller internuclear distances. Furthermore transition states appear in the PEC for magnetic-field strengths $B \gtrsim 1$ a.u.. The corresponding data, i.e., the positions and total energies of the transition states with respect to the dissociation limit, can be found in Table I. For the position of the maximum we observe a strong decrease with increasing field strength. Simultaneously the height of the maximum with respect to the dissociation energy, i.e., $E_t - \lim_{R \rightarrow \infty} E_t$, increases from 2×10^{-6} at $B = 1.0$ a.u. to 6×10^{-4} at $B = 100.0$ a.u..

We emphasize that the $^1\Sigma_g$ state is not the ground state of the hydrogen molecule in a magnetic field of arbitrary strength. In superstrong magnetic fields with $B \gtrsim 10^3$ a.u. it is well known that the $^3\Pi_u$ state represents the ground state of the hydrogen molecule [30, 37]. The ground state for magnetic-field strengths in the intermediate regime has not been investigated up to now, to our knowledge. For sufficiently weak magnetic fields the ground state has to be the $^1\Sigma_g$ state. However, we will show in section III.D that for magnetic-field strengths larger than 0.2 a.u. or equal the lowest total energy of the $^3\Sigma_u$ state is lower than the lowest total energy of the $^1\Sigma_g$ state. This means that for $B \gtrsim 0.2$ a.u. the $^3\Sigma_u$ state is the ground state of the hydrogen molecule. The “crossing field strength” of this lowest $^3\Sigma_u$ state with the $^3\Pi_u$ state, which is the ground state in superstrong magnetic fields, is not known so far.

Now let us compare our results with the few data existing in the literature. Only two investigations were performed concerning the electronic structure of the hydrogen molecule for magnetic-field strengths smaller than $B = 100$ a.u.. In Ref. [28], PECs were shown for the $^1\Sigma_g$ state for magnetic-field strengths of 0.5 a.u. and 1.0 a.u.. The authors used a very simple LCAO ansatz for the electronic wave function, including only one atomic orbital for the construction of the H_2 molecular wave function. The atomic orbitals had the following appearance: $\psi_\alpha(j) = \left(\frac{\epsilon^2}{\pi}\right)^{1/2} \exp[-\epsilon r_{\alpha j}]$ where $r_{\alpha j}$ is the distance of the α nucleus to the j th electron and ϵ is a variational parameter to be optimized. This ansatz is restricted to small magnitudes of the magnetic field ($B < 1$ a.u.) where the spherical symmetry of the $^1\Sigma_g$ wave function is approximately conserved. For magnetic-field strengths of 0.5 and 1.0 a.u., the authors of Ref. [28] provided an equilibrium distance of 1.29 a.u. corresponding to a total energy of -1.06 a.u. and an equilibrium distance

of $1.17 a.u.$ with a total energy of $-0.83 a.u.$, respectively. As shown in Table II we were able to improve these results significantly. The improvement in the total energy compared to the calculations of Ref. [28] is approximately twice as large for $B = 1.0 a.u.$ as for $B = 0.5 a.u.$. For $B = 1.0 a.u.$ the wave function of the $^1\Sigma_g$ state is deformed from a spherical one to a cylindrosymmetric one, and, therefore, a use of only one atomic orbital with a spherical symmetry is insufficient even for a qualitative description. In the second investigation performed by Turbinder [27], one of the simplest wave functions in a zero-order approximation was taken for the description of the $^1\Sigma_g$ state (see also Ref. [51]). In Table II we also compare our data with that of Ref. [27]. We observe an overall improvement of the total energy in our results compared to the data obtained by Turbinder. For a magnetic-field strength of $5.0 \times 10^9 G$ the equilibrium distance obtained by Turbinder differs significantly from our value leading to a relative difference in the total energy of 41%. We remark that the accuracy of the calculations in Ref. [27] increases with increasing magnetic-field strength. For $B = 1.0 \times 10^{11} G$ the relative improvement in the total energy obtained by our calculations amounts to only about 0.5 % compared to [27].

Finally let us investigate the question of whether vibrational levels exist in the PECs discussed above. This question is of great importance to the existence of bound states. In the presence of a magnetic field the determination of vibrational levels is a much more complicated task than in field-free space. First we note that the Born-Oppenheimer approximation known from field-free space is not valid in the presence of a magnetic field. In the presence of a magnetic field the nuclear charges are partially screened by the electrons against this field. In order to describe the partial screening of the nuclear charges against the magnetic field correctly, the diagonal term of the nonadiabatic coupling elements has to be included in the nuclear equation of motion. This leads to a new kind of adiabatic approximation, the partially screened Born-Oppenheimer approximation [42,43,52]. Furthermore, the nuclear equation of motion explicitly not only depends on the internuclear distance but also on the angle between the internuclear axis and the magnetic-field axis. The facts discussed above clearly show that the nuclear dynamics is in general very complex. Within the present framework of the parallel configuration we can therefore provide only estimations of the energy levels of the vibrational states. Nevertheless this allows us to decide whether or not we encounter physically bound states with respect to the vibrational mode R . A lower bound of the vibrational energy within our approximation is given by the lowest vibrational state in the corresponding PEC using the field-free kinetic energy $\frac{P^2}{2\mu}$. The corresponding nuclear equation of motion in field-free space for the given electronic PEC was solved with the help of a discrete variable representation [53]. The upper bound for the energy of the lowest vibrational state in the presence of a magnetic field was obtained by simply adding the Landau energy of the nuclear motion to the value of the energy obtained for the corresponding vibrational level in field-free space. In this way we obtained both upper and lower bounds for the vibrational levels. These estimations of the vibrational levels were performed for each PEC shown in Figure 1 as well as the following figures.

For the PEC of the $^1\Sigma_g$ state the procedure described above yields many, i.e., of the order of magnitude of a few dozens, of vibrational levels for the entire regime $B = 0 - 100 a.u.$ of field strengths. This means that the $^1\Sigma_g$ state is a bound state with respect to the internuclear distance R for this wide range of field strengths.

B. The $^1\Sigma_u$ state

The electronic PEC for the $^1\Sigma_u$ state in field-free space was calculated with high accuracy by Kolos and Wolniewicz [54, 55]. The energy curve in field-free space for this state possesses a minimum at an internuclear distance of $R = 2.43 a.u.$. A detailed analysis of the wave function [54] shows the predominantly ionic character of the wave function for $3 < R < 7 a.u.$. This ionic character has also been confirmed by an analysis of the corresponding rotation-vibration spectrum of the hydrogen molecule [56]. Since H^- possesses only one weakly bound state in field-free space, one expects the ionic character of the hydrogen molecule in the $^1\Sigma_u$ state to decrease with increasing internuclear distance. For large internuclear distances the wave function can be described as a mixture of $(1s\sigma 2s\sigma)$ and $(1s\sigma 2p\sigma)$ configurations, where the $(1s\sigma 2p\sigma)$ configuration predominates for very large internuclear distances. Therefore, the dissociation channel is given by $H_2 \rightarrow H(1s) + H(2p)$. The corresponding state in the united atom limit is the electronic $^3P 1s2p$ helium state. In order to check the convergence of our calculations we compared our results with the data given in Ref. [55]. The overall relative accuracy in the total energy of the present calculation for the $^1\Sigma_u$ state in field-free space is better than 10^{-3} . As can be seen from Table III our equilibrium distance differs by $0.01 a.u.$ from the correct value of $R = 2.43 a.u.$.

In the presence of a magnetic field we observe a monotonous increase in the total energy with increasing magnetic-field strength. The corresponding values are given in Table III. At the same time the dissociation energy increases monotonously (cf. Fig. 2 and Table III). It can be seen from Table III that the value of the equilibrium distance exhibits a minor increase from $2.42 a.u.$ in field-free space to $2.53 a.u.$ for $B = 0.2 a.u.$. However, for $B \geq 0.2 a.u.$ we observe a drastic decrease in the equilibrium internuclear distance with increasing magnetic-field strength. For

$B = 1.0$ and 100 a.u. , the corresponding values are $R_{eq} = 2.30$ and 0.490 a.u. , respectively. Figure 2 shows the well becoming more and more pronounced with increasing magnetic-field strength while the onset of the asymptotic convergence behavior is shifted to larger internuclear distances with increasing field strength.

Another important property of the $^1\Sigma_u$ state in a magnetic field is the change of the dissociation channel in sufficiently strong fields. As described above, the wave function in field-free space exhibits a partially ionic character for certain internuclear distances. However, the dissociation into $H^- + H^+$ is not possible due to the nonexistence of strongly bound electronic states of H^- . In a magnetic field, however, it is known that each negative ion possesses infinitely many bound states in a nonzero constant magnetic field [57,58]. This means we encounter an infinite number of bound states of H^- in the presence of a magnetic field even though H^- has only one bound state in field-free space. With increasing field strength the ground state energy of H^- shows a monotonous behavior, and H^- becomes more and more strongly bound. Consequently, there exists a critical field strength for which the total energy of the ground state of H^- and the total energy of $H(0^+) + H(0^-)$, which is the dissociation limit for weaker field strengths, are equal.

The above considerations help us to understand the asymptotic behavior in the dissociation limit of the $^1\Sigma_u$ state as well as the shape of the PEC: For magnetic-field strengths $B \lesssim 10.0 \text{ a.u.}$ the molecular $^1\Sigma_u$ state dissociates into $H(0^+) + H(0^-)$. Since the total energy of H^- is larger than the energy of $H(0^+) + H(0^-)$ and since no crossings are allowed between electronic states of the same symmetry an avoided crossing between the ground state and the first excited state in the $^1\Sigma_u$ subspace occurs in this regime of field strengths. With increasing magnetic-field strength $B = 0 \rightarrow 10 \text{ a.u.}$ the position of the avoided crossing is shifted to increasingly larger internuclear distances (for $B = 0.1$ and 10.0 a.u. the position of the crossing is at ~ 12 and 81.47 a.u. , respectively). Between $B = 10.0$ and 50.0 a.u. the dissociation channel changes from $H(0^+) + H(0^-)$ to $H_2 \rightarrow H^-(0_s^+) + H^+$, where the subscript s denotes that the H^- state is a singlet state. The “transition field strength” is approximately $B \sim 20 \text{ a.u.}$. Due to the change in the dissociation channel the onset of the asymptotic behavior of the PEC is shifted to increasingly larger internuclear distances. This leads to a totally different shape of the PEC which can be seen for $B = 100.0 \text{ a.u.}$ from Fig. 2. As a further result we obtain the ionization energy for H^- for magnetic-field strengths of $B = 50.0$ and 100.0 a.u. . The resulting total binding energies with respect to both electrons are 3.637999 a.u. and 4.561968 a.u. , respectively. The best available data for the ionization energy of the H^- -ion in a strong magnetic field $B \geq 100 \text{ a.u.}$ are given in Refs. [59,60]. Compared to the value given in Ref. [59] for $B = 100.0 \text{ a.u.}$ our result of 4.561968 a.u. is more than 1% lower in energy. The ionization energy for H^- at $B = 50.0 \text{ a.u.}$ amounts to 3.637999 a.u. and no corresponding values have been known from the literature so far.

Finally, we briefly comment on the existence of vibrational levels. Many vibrational levels were found to exist in the above PECs for arbitrary field strengths up to 100.0 a.u. . With increasing field strength the overall tendency is an increase in the number of vibrational levels.

C. The $^3\Sigma_g$ state

The Born-Oppenheimer PEC for the lowest $^3\Sigma_g$ state has been calculated with very high accuracy in field-free space. Accurate studies have been performed using explicitly correlated methods, which include wave functions of generalized James-Coolidge or Kolos-Wolniewicz type [61–63] and full CI calculations with large elliptical basis sets [64]. Our CI calculation yields 0.737124 a.u. for the total energy at the equilibrium distance of $R = 1.87 \text{ a.u.}$ (see Table IV). The relative accuracy compared to the best data available in the literature [63] amounts to 4.4×10^{-5} . We emphasize that this high precision of our data is obtained for arbitrary internuclear distances. The dissociation channel for the $^3\Sigma_g$ state in field-free space is $H_2 \rightarrow H(1s) + H(2s)$ and the helium state in the united atom limit is the $^3S 1s2s$ state.

In the presence of a magnetic field the $^3\Sigma_g$ state dissociates into $H(0^+) + H(0^-)$. The corresponding united atom state is the $^30^+$ helium state. Due to the spin-Zeeman shift the total energy monotonously decreases with increasing magnetic-field strength as can be seen in Table IV. For magnetic-field strengths below 0.5 a.u. we observe a monotonous decrease in the dissociation energy E_{d1} with increasing magnetic-field strength from 0.112124 to 0.062317 a.u. for $B = 0.0$ and 0.5 a.u. , respectively. At the same time the equilibrium distance decreases slightly from 1.87 a.u. to 1.81 a.u. . For magnetic-field strengths larger than 0.5 a.u. we observe a drastic increase in the dissociation energy and a simultaneous decrease in the equilibrium internuclear distance. Detailed numerical data for the PEC are provided in Table IV and the development of the electronic PEC for internuclear distances smaller than 4.0 a.u. is illustrated in Fig.3. In Fig. 3 we can observe that the well of the PEC becomes increasingly more shallow for increasing field strengths in the range $B = 0.0 \rightarrow 0.5 \text{ a.u.}$. With further increasing magnetic-field strength the opposite behavior can be observed and the potential well becomes more and more pronounced and deeper.

A closer look at the PEC reveals that for magnetic-field strengths between 0.05 and 50.0 a.u. the $^3\Sigma_g$ state develops a second minimum, which has no counterpart in field-free space. However, this minimum is very shallow and the

maximum dissociation energy amounts to only $1.91 \times 10^{-3} a.u.$ at a magnetic-field strength of $1.0 a.u.$. From Table IV we see the dependence of the dissociation energy and the equilibrium internuclear distance of this second minimum on the magnetic-field strength. The corresponding PECs are shown in Fig.4. In this figure we observe a hump of the ${}^3\Sigma_g$ state at $B = 0.05 a.u.$. This hump also occurs for higher magnetic-field strengths, but is shifted to smaller internuclear distances and, therefore cannot be seen in Fig. 4. For the location of the maximum we observe an overall decrease in the internuclear distance with increasing magnetic-field strength. Numerical data concerning the position and total energy of the maximum in the energy curve are also given in Table IV. Both the maximum and second minimum of the PEC appear at the same magnetic-field strength of $0.05 a.u.$. However, the second minimum vanishes for magnetic-field strengths larger than $50.0 a.u.$ whereas the hump remains in the PEC.

Let us finally focus on the existence of vibrational levels. For the first minimum we found in the order of ten vibrational levels. The number of levels slightly decreases from $B = 0.0$ to $0.5 a.u.$ with decreasing depth of the well. For larger field strengths ($5.0, 10.0,$ and $100.0 a.u.$) the number of levels slightly increases again. For the second, i.e., outer, minimum we found about five vibrational levels for the field strengths $0.05, 0.2,$ and $1.0 a.u.$, respectively. For a field strength $B = 5.0 a.u.$ the lower bound of the vibrational energy lies inside the potential well whereas the upper bound is above the well. Here the detailed dynamical behavior decides on the existence of vibrational levels, and no definite conclusion can be drawn from our estimations. For $B = 50.0 a.u.$ the same conclusion holds.

D. The ${}^3\Sigma_u$ state

In field-free space the electronic PEC of the ${}^3\Sigma_u^+$ state is repulsive, i.e., does not exhibit a well-pronounced potential well. The united atom limit of this state is the ${}^3S 1s2p$ helium state, and the dissociation channel is $H_2 \rightarrow H(1s) + H(1s)$. One of the early but very accurate Born-Oppenheimer calculations on the lowest ${}^3\Sigma_u^+$ state was performed by Kolos and Wolniewicz [65,66]. Recently several calculations were performed in order to improve the Born-Oppenheimer potential energy for this state [64,67–69]. Most accurate results were obtained using a Hylleraas-type expansion [65,66], explicitly correlated Cartesian Gaussian basis functions [68], or elliptical basis functions [64].

As a reference for our calculations we used the data given in Ref. [64] for internuclear distances smaller than $4.0 a.u.$ and Refs. [65,66] for $R \geq 4.0 a.u.$. For $R \leq 4a.u.$ we obtained an overall relative accuracy of 6×10^{-4} compared to the results in Ref. [64]. For larger values of the internuclear distance this accuracy further increases, and we obtained a relative accuracy of at least 3×10^{-6} . The best conventional CI calculations for this state with a basis set of spherical Gaussian-type orbitals were performed in Ref. [69]. Comparing our results with the data given in Ref. [69] it can be seen that our values of the total energy are lower by 1.0% and 0.4% for $R \leq 2.0$ and $R \geq 2.0$, respectively. Our accurate results, in particular for the ${}^3\Sigma_u^+$ state in field-free space demonstrate the usefulness of our basis set of nonspherical nonorthogonal Cartesian Gaussian basis functions. The PEC for the ${}^3\Sigma_u^+$ state for different magnetic-field strengths is presented in Fig.5.

Despite the fact that the PEC of the ${}^3\Sigma_u^+$ state is predominantly repulsive it exhibits a very shallow van der Waals minimum around $R \sim 8 a.u.$. Due to the dissociation of the ${}^3\Sigma_u^+$ state into $H(1s) + H(1s)$, we encounter a dipole-dipole interaction of induced dipole moments for large internuclear distances which is proportional to $\frac{1}{R^6}$. The PEC in the vicinity of the van der Waals minimum is presented in Fig.6, and numerical data are given in Table V. For the van der Waals minimum we obtained a dissociation energy of $1.885 \times 10^{-5} a.u.$ at an internuclear distance of $7.9 a.u.$. The determination of the van der Waals energy and the corresponding minimum is a delicate task and requires very large basis sets as well as high numerical accuracy. Within our calculations the position of the minimum has been determined with 'only' two significant digits. Since the dissociation energy is very small the relative accuracy of our result of the dissociation energy differs from the high precision calculations in Refs. [65,66] by about 17%. We emphasize that the description of the van der Waals minimum is a drastic improvement compared to the results of Ref. [69] where no minimum was predicted.

In the following we discuss the development of the PEC for the ${}^3\Sigma_u^+$ state depending on the magnetic-field strength. First, we focus on the global structure which is shown in Fig. 5. In the presence of a magnetic field the separated atom limit is given by $H_2 \rightarrow H(0^+) + H(0^+)$, i.e., the molecule dissociates into two hydrogen atoms in their ground states with positive z parity. The corresponding united atom state in the presence of a magnetic field is the ${}^30^-$ helium state. First of all we mention that the onset of the asymptotic behavior with respect to the dissociation occurs for increasingly smaller internuclear distances with increasing magnetic-field strength. A comparison of the energy values given in Tables I and Table V reveals that for magnetic-field strengths larger than $0.2 a.u.$ the ${}^3\Sigma_u$ state is lower in energy than the ${}^1\Sigma_g$ state. Therefore, the crossing between these two states happens between the two field strengths 0.1 and $0.2 a.u.$. In Fig. 7 and Fig. 8 we illustrate the crossing of these two states. In Fig. 7, which shows the total energy of the ${}^1\Sigma_g$ and ${}^3\Sigma_u$ states at a magnetic-field strength of $B = 0.0 a.u.$, we can see the ${}^3\Sigma_u$ state being higher in the total energy as the ${}^1\Sigma_g$ state. Figure 8 shows the same states at a magnetic-field strength of

$B = 0.5 \text{ a.u.}$. In this figure we observe a drastic decrease in the total energy of the ${}^3\Sigma_u$ state. The crossing of these two states has an important consequence for the stability of molecular hydrogen in astrophysics. Beyond $B \sim 0.2 \text{ a.u.}$ the ground state of the hydrogen molecule is the ${}^3\Sigma_u$ state which is an unbound electronic state at least for the parallel configuration. It is a challenging task to clarify whether this is true for any angle of the internuclear axis with respect to the magnetic-field axis. In principle it is possible that a potential well might develop if the internuclear and magnetic-field axes do not coincide. The investigation of such configurations is an important task in the future. In addition we mention that beyond $B \gtrsim 3 \times 10^3 \text{ a.u.}$ the global ground state of H_2 is the ${}^3\Pi_u$ state [18,30].

In the following we investigate the development of the van der Waals minimum depending on the magnetic-field strength which is of particular interest for the determination of the global ground state of the hydrogen molecule in a magnetic field. In field-free space the van der Waals potential is given by a law proportional $\frac{1}{R^6}$ due to the dipole-dipole interaction of induced dipoles in first order perturbation theory. In the presence of a magnetic field we have to pay attention to another interaction between atoms in s states. In first-order perturbation theory two atoms in a magnetic field interact like two permanent quadrupoles. Therefore the leading expression in first-order perturbation theory is proportional to $\frac{1}{R^5}$. In Fig. 6 we show the development of the van der Waals minimum with increasing magnetic-field strength. As can be seen from Table V the dissociation energy increases by $0.175 \times 10^{-5} \text{ a.u.}$ if we increase the field strength from zero to 0.2 a.u. . At the same time we observe a monotonous decrease of the internuclear distance corresponding to the minimum from 7.9 to 7.7 a.u. . In Fig. 6 we observe that the shape of the energy curve for $B = 0.2 \text{ a.u.}$ differs only slightly from that in field-free space. For magnetic-field strengths larger than $B = 0.2$ the dissociation energy decreases drastically with increasing magnetic-field strength down to 0.375×10^{-5} for $B = 1.0 \text{ a.u.}$. Simultaneously the energy curve changes its shape. The gradient of the energy with respect to internuclear distances $R \leq R_{eq}$ becomes larger and a more and more shallow minimum can be observed. For magnetic-field strengths larger than 1.0 a.u. no minimum is observed. The gradient of the energy with respect to the internuclear distance increases further with increasing magnetic-field strength, changing the appearance of the PEC to an increasingly flatter curve. No vibrational levels were found for any field strength.

Finally we draw the readers attention to the fact that the calculations concerning the position and dissociation energy of the van der Waals minimum are close to the convergence limit of our calculations. The disappearance of the van der Waals minimum within our calculations to our opinion reflects a real physical effect, but needs further investigation for a definite clarification. In order to answer the question about the lowest bound state of the hydrogen molecule in the high field regime, a detailed and very accurate investigation of the ${}^3\Pi_u$ electronic state has to be performed.

IV. SUMMARY AND CONCLUSIONS

In the present paper we investigated the electronic structure of the hydrogen molecule in a magnetic field. We hereby focused on the case of a parallel internuclear axis and a magnetic-field axis for a magnetic quantum number equal to zero. The key ingredient for our CI calculations is a basis set of nonorthogonal nonspherical Gaussian atomic orbitals which was established previously. The corresponding basis sets can be obtained from the authors upon request. Our results for the PECs in field-free space show a high accuracy compared to the existing data in the literature. The non-spherical atomic orbitals may therefore be very useful for precision calculations concerning molecules in field-free space.

First we investigated the lowest ${}^1\Sigma_g$ state which is the ground state of the hydrogen molecule in field-free space. In the presence of a magnetic field we observed a monotonous increase in the total energy. At the same time the equilibrium distance decreases and the dissociation energy (chemical binding energy) increases rapidly. The few existing data concerning the total energy of the ${}^1\Sigma_g$ state in the presence of a magnetic field were significantly improved by our calculations. By calculating lower and upper bounds for the lowest vibrational energy the PEC of the ${}^1\Sigma_g$ state was shown to contain many vibrational levels for any magnetic-field strength up to 100 a.u. .

In the next step we studied the lowest state in the ${}^1\Sigma_u$ subspace. With increasing magnetic field we first observed a minor increase in the equilibrium internuclear distance in the range $0.0 \leq B \leq 0.2 \text{ a.u.}$. The dissociation and the total energy increases monotonously with increasing magnetic-field strength. Many vibrational levels were found for the PEC of the ${}^1\Sigma_u$ state in the entire regime $B = 0 - 100 \text{ a.u.}$. The number of levels hereby increase with increasing field strength. An important feature of the ${}^1\Sigma_u$ state is the change in the dissociation channel with increasing magnetic-field strength. In field-free space we have $H_2 \rightarrow H(1s) + H(2p)$ in the separated atom limit. The wave function possesses a predominantly ionic character for large values of the internuclear distance. However, in field-free space the dissociation $H_2 \rightarrow H^- + H^+$ of the lowest ${}^1\Sigma_u$ state is not possible due to the nonexistence of strongly bound states for the H^- -ion in field-free space. In contrast to this strongly bound states of H^- exist in the presence of a magnetic field. Therefore a dissociation into $H^- + H^+$ is possible and we observe a change in the dissociation channel

for magnetic-field strengths between $B = 10.0$ and 50.0 *a.u.*: For $B \leq 10.0$ *a.u.* we have $H_2 \rightarrow H(0^+) + H(0^-)$. For field strengths slightly larger than 10.0 *a.u.* the dissociation limit is given by $H_2 \rightarrow H^-(0_s^+) + H^+$. As a result of our calculations we therefore obtained the dissociation energy for H^- for $B = 50.0$ and 100.0 *a.u.*. Our result of 4.561968 *a.u.* for the ionization energy for H^- at $B = 100.0$ *a.u.* shows an improvement of more than one % compared to the best value given in the literature.

For the $^3\Sigma_g$ state we encounter a monotonous decrease in the total energy which is proportional to the field strength, and which arises due to the spin-Zeeman shift in the presence of a magnetic field. In the range $0.0 \leq B \leq 0.5$ *a.u.* the dissociation energy decreases approximately by a factor of two compared to the dissociation energy in field-free space. Simultaneously the equilibrium internuclear distance decreases slightly from 1.87 to 1.81 *a.u.*. With further increasing magnetic-field strength we observe a drastical increase in the dissociation energy and a simultaneous decrease of the internuclear equilibrium distance. A more detailed investigation of the PEC for the $^3\Sigma_g$ state shows a second minimum for magnetic-field strengths between 0.05 and 50.0 *a.u.* which has no counterpart in field-free space. However, this additional minimum is very shallow. Vibrational levels were found to exist within the first well of the PEC for the entire range of field strengths from $B = 0$ to 100 *a.u.*. For the second minimum for field strengths $B \gtrsim 5$ *a.u.* the existence of vibrational levels depends on the detailed dynamical behavior and cannot be decided within the present approach. For $B \lesssim 5$ *a.u.* a few vibrational levels exist.

Finally we investigated the lowest $^3\Sigma_u$ state of the hydrogen molecule which is known to be repulsive in field-free space and possesses only a very shallow van der Waals minimum at $R \sim 8.0$ *a.u.*. The repulsive character of the PEC of the $^3\Sigma_u$ state remains for arbitrary field strengths up to $B = 100.0$ *a.u.*. Due to the spin-Zeeman shift in a magnetic field a crossing occurs between the $^1\Sigma_g$ and $^3\Sigma_u$ state in the range $0.1 \leq B \leq 0.2$ *a.u.*. Therefore the lowest state of the Σ subspace of the hydrogen molecule in the presence of a magnetic field is the $^1\Sigma_g$ state for $B \leq 0.1$ *a.u.* and the $^3\Sigma_u$ state for $B \geq 0.2$ *a.u.*. In superstrong magnetic fields $B \gtrsim 3 \times 10^3$ *a.u.* the ground state is the $^3\Pi_u$ state. The determination of the crossing of the $^3\Sigma_u$ and $^3\Pi_u$ states is a task which is left to a future investigation. Furthermore the nonexistence of a strongly bound ground state of the hydrogen molecule has to be confirmed by investigations concerning arbitrary angles between the internuclear axis and magnetic-field axis. After considering these general properties of the $^3\Sigma_u$ state we investigated the development of the van der Waals minimum depending on the field strength. For the van der Waals minimum we observe a monotonous decrease in the equilibrium internuclear distance with increasing field strength. First the dissociation energy increases with increasing field strength and for $B \geq 0.5$ *a.u.* the dissociation energy drastically decreases. For $B \geq 1.0$ *a.u.* no minimum has been found. No vibrational levels exist for any field strength up to 1 *a.u.*.

The existence of a minimum which supports a vibrational frequency for the lowest electronic state of the hydrogen molecule for intermediate magnetic-field strengths is of particular interest to astrophysics in order to determine whether hydrogen molecules exist in the vicinity of white dwarfs. According to our investigations for $B \gtrsim 0.2$ *a.u.* the ground state of the hydrogen molecule is not strongly bound and exhibits only a weak minimum due to the van der Waals interaction. However, in superstrong magnetic fields the ground state is strongly bound, and the crossing between these two states is not known so far. Finally we emphasize that for drawing definite conclusions about the existence or nonexistence of a potential well, the case of nonparallel internuclear axis and magnetic-field axis has to be investigated. The determination of the corresponding potential energy surfaces is a complicated task which is left to future investigations.

V. ACKNOWLEDGMENTS

The Deutsche Forschungsgemeinschaft as well as the European Community (F. K. D.) are gratefully acknowledged for financial support. We thank U. Kappes for fruitful discussions. Computer time was generously provided by the Rechenzentrum Heidelberg, and in particular by the Rechenzentrum Karlsruhe.

APPENDIX A: CONSTRUCTION OF THE MOLECULAR ELECTRONIC WAVE FUNCTION

In order to construct the spatial part of the electronic wave function for the hydrogen molecule we first establish the molecular orbitals Φ_i for the H_2^+ ion. The construction of these orbitals was described in detail in Ref. [23]. The molecular electronic wave functions for the H_2^+ -ion read as follows:

$$\psi^{\pm m, p} = \sum_k c_k \Phi_k^{\pm m, p}(\mathbf{r}, \alpha_k, \beta_k, R)$$

$$= \sum_k c_k \sum_a^{|m|} \sum_b^N \binom{|m|}{a} \binom{N}{b} (\pm i)^a \left[\phi_{\mathbf{n}_{ab,k}}(\mathbf{r}, \alpha_k, \beta_k, +R/2) + (-1)^{P+P_{a,k}} \phi_{\mathbf{n}_{ab,k}}(\mathbf{r}, \alpha_k, \beta_k, -R/2) \right] \quad (\text{A1})$$

Each molecular orbital Φ_i is an eigenfunction to the molecular angular momentum operator L_z and to the molecular parity operator P of the H_2^+ -ion. Therefore, the H_2^+ orbitals Φ_i are labeled by the eigenvalues $\pm m$ of L_z and the eigenvalues $p = \pm 1$ of P . P_a is the parity operator of the atomic orbital and c_i denote the expansion coefficients. The atomic orbitals ϕ building the molecular orbitals Φ have the following structure:

$$\phi_{\mathbf{n}_{ab,k}}(\mathbf{r}, \alpha_k, \beta_k, \pm R/2) = x^{n_x, ab, k} y^{n_y, ab, k} (z \mp R/2)^{n_z, ab, k} \exp \left\{ -\alpha_k (x^2 + y^2) - \beta_k (z \mp R/2)^2 \right\}, \quad (\text{A2})$$

where α_k and β_k are optimized variational parameters [39]. R represents the internuclear distance and $\mathbf{r}^T = (x, y, z)$ the electronic position vector. For the dependencies of the powers n_x, n_y , and n_z on the atomic magnetic quantum number, we refer the reader to Ref. [23]. Now we are able to describe the molecular electronic wave function by a linear combination of products of these H_2^+ orbitals. First, we have to ensure that the H_2 molecular orbitals are eigenfunctions to the molecular angular momentum operator L_z of H_2 . Therefore, we arrive at the condition $M = m_1 + m_2$ for the magnetic quantum numbers m_1 and m_2 characterizing the two H_2^+ orbitals. Moreover, the H_2 molecular orbitals have to be eigenfunctions to the molecular parity operator P_g of the H_2 molecule and the total molecular electronic wave function has to respect the Pauli principle. Therefore, the electronic wave function of the hydrogen molecule reads as follows:

$$\Psi^{M, P_g} = \sum_{i,j} c_{ij} \left\{ \Phi_i^{\pm m_1, \pm 1}(\mathbf{r}_1, \alpha_i, \beta_i, R) \Phi_j^{\pm m_2, \pm 1}(\mathbf{r}_2, \alpha_j, \beta_j, R) \pm \Phi_i^{\pm m_1, \pm 1}(\mathbf{r}_2, \alpha_i, \beta_i, R) \Phi_j^{\pm m_2, \pm 1}(\mathbf{r}_1, \alpha_j, \beta_j, R) \right\} \\ + c'_{ij} \left\{ \Phi_i^{\pm m_1, \mp 1}(\mathbf{r}_1, \alpha_i, \beta_i, R) \Phi_j^{\pm m_2, \mp 1}(\mathbf{r}_2, \alpha_j, \beta_j, R) \pm \Phi_i^{\pm m_1, \mp 1}(\mathbf{r}_2, \alpha_i, \beta_i, R) \Phi_j^{\pm m_2, \mp 1}(\mathbf{r}_1, \alpha_j, \beta_j, R) \right\} \quad (\text{A3})$$

with

$$\Phi_i^{\pm m_1, \pm 1}(\mathbf{r}_{1,2}, \alpha_i, \beta_i, R) = \sum_i c_i \sum_a^{|m_1|} \sum_b^N \binom{|m_1|}{a} \binom{N}{b} (\pm i)^a \times \\ \left[\phi_{\mathbf{n}_{ab,i}}(\mathbf{r}_{1,2}, \alpha_i, \beta_i, +R/2) + (-1)^{P_1+P_{a,i}} \phi_{\mathbf{n}_{ab,i}}(\mathbf{r}_{1,2}, \alpha_i, \beta_i, -R/2) \right] \quad (\text{A4})$$

and

$$\Phi_j^{\pm m_2, \pm 1}(\mathbf{r}_{1,2}, \alpha_j, \beta_j, R) = \sum_j c_j \sum_a^{|m_2|} \sum_b^{N'} \binom{|m_2|}{a} \binom{N'}{b} (\pm i)^a \times \\ \left[\phi_{\mathbf{n}_{ab,j}}(\mathbf{r}_{1,2}, \alpha_j, \beta_j, +R/2) + (-1)^{P_g+P_2+P_{a,j}} \phi_{\mathbf{n}_{ab,j}}(\mathbf{r}_{1,2}, \alpha_j, \beta_j, -R/2) \right] \quad (\text{A5})$$

In order to ensure that the molecular wave function (A3) is an eigenfunction to the molecular parity operator P_g we multiplied the second atomic orbital $\phi_{\mathbf{n}_{ab,j}}$ in Eq. (A5) by an additional factor of $(-1)^{P_g}$.

In Eq. (A3) we have to pay attention to the special case when two atomic orbitals belonging to the molecular orbitals Φ_i , Eq. (A4), and Φ_j , Eq. (A5), are equal. For both wave functions with ungerade symmetry ($^1\Sigma_u$ and $^3\Sigma_u$) only one combination of H_2^+ orbitals in eq.(A3) contributes to the total wave function. In that case the two expressions in parenthesis are linear dependent, i.e., they are equal except for a multiplication factor of $+1$ or -1 for the $^1\Sigma_u$ and $^3\Sigma_u$ states, respectively. For the $^3\Sigma_g$ state we have no contribution to the total wave function since the two expressions in parentheses both equal zero due to the Pauli principle.

APPENDIX B: EVALUATION OF THE MATRIX ELEMENTS

Let us introduce the abbreviation:

$$\Phi_i(\mathbf{r}) := \Phi_i^{\pm m_1, \pm 1}(\mathbf{r}, \alpha_i, \beta_i, R) \quad (\text{B1})$$

with the H_2^+ orbitals Φ_i given in Appendix A. The following matrix elements have to be evaluated:

$$\int d\mathbf{r}_1 \Phi_i(\mathbf{r}_1) \Phi_k(\mathbf{r}_1) \quad (\text{B2})$$

$$\int d\mathbf{r}_1 \Phi_i(\mathbf{r}_1) \left\{ \mathbf{p}_1 - \frac{1}{2}(\mathbf{B} \times \mathbf{r}_1) \right\}^2 \Phi_k(\mathbf{r}_1) \quad (\text{B3})$$

$$\int d\mathbf{r}_1 \Phi_i(\mathbf{r}_1) \frac{1}{|\mathbf{r}_1 \pm R/2|} \Phi_k(\mathbf{r}_1) \quad (\text{B4})$$

$$\int d\mathbf{r}_1 d\mathbf{r}_2 \Phi_i(\mathbf{r}_1) \Phi_j(\mathbf{r}_2) \frac{1}{|\mathbf{r}_1 - \mathbf{r}_2|} \Phi_k(\mathbf{r}_1) \Phi_l(\mathbf{r}_2) \quad (\text{B5})$$

All these integrals are evaluated in Cartesian coordinates. For the simple overlap matrix elements in eq.(B2) a closed-form analytical expression can be given which has been implemented and optimized with respect to the numerical performance. The matrix elements for the kinetic, paramagnetic, and diamagnetic operator in Eq. (B3) can be reduced to simple overlap matrix elements eq.(B2).

The evaluation of the electron-nucleus (Eq. B4) and electron-electron (Eq. B5) integrals is much more complicated. First, one has to regularize the singularities. This is done by the following transformation at the expense of an additional integration [70]:

$$\begin{aligned} \frac{1}{f(\mathbf{r})} &= \pi^{-1/2} \int_{-\infty}^{+\infty} \exp[-u^2 f^2(\mathbf{r})] du \\ &= \frac{2}{\pi^{1/2}} \int_0^1 \exp\left[-f^2(\mathbf{r}) \frac{v^2}{1-v^2}\right] \frac{dv}{(1-v^2)^{3/2}} \end{aligned} \quad (\text{B6})$$

In our case, $f(\mathbf{r})$ equals $|\mathbf{r}_1 \pm R/2|$ for the electron-nucleus integral or $|\mathbf{r}_1 - \mathbf{r}_2|$ for the electron-electron integral, respectively.

In the case of the electron-nucleus integral, we first perform the integration over the electronic coordinates. This integration is done by a special kind of exact quadrature, the so-called Rys quadrature [71, 72]. The Rys quadrature has been proved to be very useful for the fast calculation of two electron integrals, in particular for higher angular momenta of the involved orbitals [73, 74]. We emphasize that this quadrature technique yields the exact result for the integration. Only one integration over the u coordinate remains to be done. This last integration is performed by a numerical algorithm. We herefore used a modified Clenshaw-Curtis quadrature based on a CERN library called 'CHEBQU'. In order to enhance the performance of our calculations, the algorithm of this routine was rewritten in the following way: Normally the routine is intended to perform one integration at each step. The molecular orbitals Φ_i in Eqs. (B2), (B3), (B4), (B5) are constructed by means of different atomic orbitals ϕ_n in Cartesian coordinates (A2). Within these integrals, only the powers of the polynomials in the electronic x and y coordinates change but the power of the z coordinate remains the same. It is therefore useful to perform all integrals over Cartesian coordinates belonging to a molecular orbital Φ_i in one step. We hereby avoid the repeated numerical integration of identical integrals. For the special case of sufficiently small powers of the z -coordinate we implemented explicitly the analytical solutions of the integration over the z coordinate, i.e., we implemented 60 different functions for the different z -integrations. For a matrix with a dimension of 3500 we are able to evaluate all integrals of the forms Eqs. (B2),(B3), (B4) within six seconds of CPU time on an AIX 590 computer.

The electron-electron integrals are the most difficult ones to solve. Again we first remove the singularity of the integrand by transformation (B6). Subsequently six integrations over the electronic coordinates are performed with the Rys quadrature technique. In total this corresponds to a rather lengthy calculation. Finally the last integration is again done with a modified Clenshaw-Curtis quadrature. Following these steps for the evaluation of the electron-electron integrals leads to serious trouble. Integrals centered at different nuclei turn out to possess very similar values. In fact, many numerically evaluated integrals are identical within the accuracy of our numerical integration. Therefore, if we simply add the results of different integrals, the desirable accuracy is easily lost. To avoid this problem the corresponding integrands have been combined in a suitable manner: Instead of adding the results of different integrals we added the integrands and then numerically performed the integration. We hereby got rid of the accuracy problems. Due to the new kind of integrands the termination condition of the standard Clenshaw-Curtis quadrature proved to

be no longer valid. We therefore implemented a new criterion to ensure the convergence of our numerical integration. Similar to the electron-nucleus integrals we used a variety of different functions for the special cases of the second z integration. The size of the program package for the evaluation of the electron-electron and electron-nucleus integrals (programming language C) amounts to 12000 lines.

- [1] J. P. Ostriker and F. D. A. Hartwick, *Astrophys. J.* **153**, 797 (1968).
- [2] J. Kemp, J. S. Swedlund, J. Landstreet, and J. Angel, *Astrophys. J.* **161**, L77 (1970).
- [3] J. Trümper *et al.*, *Ann. N. Y. Acad. Sci.* **302**, 538 (1977).
- [4] S. T. Chiu, *Phys. Rev. B* **9**, 3438 (1974).
- [5] M. L. Glasser and J. I. Kaplan, *Astrophys. J.* **199**, 208 (1975).
- [6] E. G. Flowers *et al.*, *Astrophys. J.* **215**, 291 (1977).
- [7] E. Müller, *Astron. Astrophys.* **130**, 415 (1984).
- [8] I. Fushiki, E. H. Gudmundsson, C. J. Pethik, and J. Yngvason, *Ann. Phys. (NY)* **216**, 29 (1992).
- [9] A. M. Abrahams and S. L. Shapiro, *Astrophys. J.* **382**, 233 (1992).
- [10] E. H. Lieb, J. P. Solovej, and J. Yngvason, *Phys. Rev. Lett.* **69**, 749 (1992).
- [11] R. O. Müller, A. R. P. Rau, and L. Spruch, *Phys. Rev. Lett.* **26**, 1136 (1971).
- [12] P. B. Jones, *Mon. Not. R. Astr. Soc.* **216**, 503 (1985).
- [13] P. B. Jones, *Phys. Rev. Lett.* **55**, 1338 (1986).
- [14] J. Virtamo, *J. Phys. B* **9**, 751 (1976).
- [15] P. Pröschel *et al.*, *J. Phys. B* **15**, 1959 (1982).
- [16] D. Neuhauser, S. E. Koonin, and K. Langanke, *Phys. Rev. A* **36**, 4163 (1987).
- [17] M. C. Miller and D. Neuhauser, *Mon. Not. R. Astr. Soc.* **253**, 107 (1991).
- [18] D. Lai, E. E. Salpeter, and S. L. Shapiro, *Phys. Rev. A* **45**, 4832 (1992).
- [19] H. Ruder, G. Wunner, H. Herold, and F. Geyer, *Atoms in strong magnetic fields* (Springer-Verlag, Berlin, 1994).
- [20] U. Wille, *Phys. Rev. A* **38**, 3210 (1988).
- [21] U. Kappes, P. Schmelcher, and T. Pacher, *Phys. Rev. A* **50**, 3775 (1994).
- [22] U. Kappes and P. Schmelcher, *J. Chem. Phys.* **100**, 2878 (1994).
- [23] U. Kappes and P. Schmelcher, *Phys. Rev. A* **51**, 4542 (1995).
- [24] U. Kappes and P. Schmelcher, *Phys. Rev. A* **53**, 3869 (1996).
- [25] U. Kappes and P. Schmelcher, *Phys. Rev. A* **54**, 1313 (1996).
- [26] U. Kappes and P. Schmelcher, *Phys. Lett. A* **210**, 409 (1996).
- [27] A. V. Turbiner, *Pis'ma Zh. Eksp. Teor. Fiz.* **38**, 510 (1983), [*JETP Lett.* **38**, 618 (1983)].
- [28] S. Basile, F. Trombetta, and G. Ferrante, *Nuovo Cimento* **9**, 457 (1987).
- [29] T. S. Monteiro and K. T. Taylor, *J. Phys. B* **23**, 427 (1990).
- [30] G. Ortiz, M. D. Jones, and D. M. Ceperley, *Phys. Rev. A* **52**, R3405 (1995).
- [31] D. Lai and E. E. Salpeter, *Phys. Rev. A* **53**, 152 (1996).
- [32] A. V. Korolev and M. A. Liberman, *Phys. Rev. A* **45**, 1762 (1992).
- [33] A. V. Korolev and M. A. Liberman, *Physica A* **193**, 347 (1993).
- [34] A. V. Korolev and M. A. Liberman, *Phys. Rev. B* **47**, 14318 (1993).
- [35] A. V. Korolev and M. A. Liberman, *Phys. Rev. Lett.* **72**, 270 (1994).
- [36] A. V. Korolev and M. A. Liberman, *Phys. Rev. Lett.* **74**, 4096 (1995).
- [37] D. Lai, *Phys. Rev. Lett.* **74**, 4095 (1995).
- [38] P. Schmelcher and L. S. Cederbaum, *Phys. Rev. A* **41**, 4936 (1990).
- [39] P. Schmelcher and L. S. Cederbaum, *Phys. Rev. A* **37**, 672 (1988).
- [40] B. Johnson, J. Hirschfelder, and K. Yang, *Rev. Mod. Phys.* **55**, 109 (1983).
- [41] J. E. Avron, I. W. Herbst, and B. Simon, *Ann. Phys.* **114**, 431 (1978).
- [42] P. Schmelcher, L. S. Cederbaum, and H.-D. Meyer, *Phys. Rev. A* **38**, 6066 (1988).
- [43] P. Schmelcher, L. S. Cederbaum, and U. Kappes, in *"Conceptual Trends in Quantum Chemistry"*, edited by Eugene S. Kryachko (Kluwer Academic Publishers, Dordrecht, 1994).
- [44] P. Schmelcher, L. S. Cederbaum, and H.-D. Meyer, *J. Phys. B* **21**, L445 (1988).
- [45] A. D. McLean, A. Weiss, and M. Yoshimine, *Rev. Mod. Phys.* **32**, 211 (1960).
- [46] H. M. James and A. S. Coolidge, *J. Chem. Phys.* **1**, 825 (1933).
- [47] W. Kolos, *J. Chem. Phys.* **101**, 1330 (1994).
- [48] L. Wolniewicz, *J. Chem. Phys.* **103**, 1792 (1995).
- [49] E. R. Davidson and L. L. Jones, *J. Chem. Phys.* **37**, 1918 (1962).

- [50] M. Demeur, P. H. Heenen, and M. Godefroid, *Phys. Rev. A* **49**, 176 (1994).
- [51] F. Dyson, *Phys. Rev.* **85**, 631 (1952).
- [52] T. Detmer, P. Schmelcher, and L. S. Cederbaum, *J. Phys. B* **28**, 2903 (1995).
- [53] D. T. Colbert and W. H. Miller, *J. Chem. Phys.* **96**, 1982 (1992).
- [54] W. Kolos and L. Wolniewicz, *J. Chem. Phys.* **45**, 509 (1966).
- [55] W. Kolos and L. Wolniewicz, *J. Chem. Phys.* **48**, 3672 (1968).
- [56] G. Herzberg and L. L. Howe, *Can. J. Phys.* **37**, 636 (1959).
- [57] J. E. Avron, I. W. Herbst, and B. Simon, *Commun. Math. Phys.* **79**, 529 (1981).
- [58] J. Fröhlich, E. H. Lieb, and M. Loss, *Commun. Math. Phys.* **104**, 251 (1986).
- [59] M. Vincke and D. Baye, *J. Phys. B* **22**, 2089 (1989).
- [60] D. M. Larsen, *Phys. Rev. B* **20**, 5217 (1979).
- [61] W. Kolos, *Chem. Phys. Lett.* **31**, 43 (1975).
- [62] W. Kolos and J. Rychlewski, *Chem. Phys. Lett.* **59**, 183 (1978).
- [63] D. M. Bishop and L. M. Cheung, *Chem. Phys. Lett.* **79**, 130 (1981).
- [64] J. W. Liu and S. Hagstrom, *J. Phys. B* **27**, L729 (1994).
- [65] W. Kolos and L. Wolniewicz, *J. Chem. Phys.* **43**, 2429 (1965).
- [66] W. Kolos and L. Wolniewicz, *Chem. Phys. Lett.* **24**, 457 (1974).
- [67] J. W. Liu and S. Hagstrom, *Phys. Rev. A* **48**, 166 (1993).
- [68] D. Frye, G. C. Lie, and E. Clementi, *J. Chem. Phys.* **91**, 2366 (1989).
- [69] F. Borondo, F. Martin, and M. Yanez, *J. Chem. Phys.* **86**, 4982 (1986).
- [70] K. Singer, *Proc. R. Soc. London, Ser. A* **402**, 412 (1960).
- [71] G. Szegő, *Orthogonal Polynomials* (American Mathematics Society, New York, 1959).
- [72] H. F. King and M. Dupuis, *J. Comp. Phys.* **21**, 122 (1976).
- [73] M. Dupuis, J. Rys, and H. F. King, *J. Chem. Phys.* **65**, 111 (1965).
- [74] M. Dupuis, J. Rys, and H. F. King, *QCPE* **338**, HONDO (1976).

FIG. 1. PECs for $B = 0.0, 1.0, 10.0$ and 100.0 *a.u.* for the lowest $^1\Sigma_g$ state ; the energy is shown with respect to the dissociation limit i.e., $E(R) = E_t(R) - \lim_{R \rightarrow \infty} E_t(R)$

FIG. 2. PECs for $B = 0.0, 1.0, 10.0$ and 100.0 *a.u.* for the lowest $^1\Sigma_u$ state; the energy is shown with respect to the dissociation limit i.e., $E(R) = E_t(R) - \lim_{R \rightarrow \infty} E_t(R)$

FIG. 3. PECs for $B = 0.0, 0.5, 5.0, 10.0$ and 100.0 *a.u.* in the range $0.1 < R < 4$ *a.u.* for the lowest $^3\Sigma_g$ state showing the first minimum of this state ; the energy is shown with respect to the dissociation limit i.e., $E(R) = E_t(R) - \lim_{R \rightarrow \infty} E_t(R)$

FIG. 4. PECs for $B = 0.05, 0.2, 1.0, 5.0$ and 50.0 *a.u.* in the range $6 < R < 15$ *a.u.* illustrating the second minimum of the lowest $^3\Sigma_g$ state; the energy is shown with respect to the dissociation limit i.e., $E(R) = E_t(R) - \lim_{R \rightarrow \infty} E_t(R)$

FIG. 5. PECs for $B = 0.0, 1.0, 10.0$ and 100.0 *a.u.* for the lowest $^3\Sigma_u$ state; the energy is shown with respect to the dissociation limit i.e., $E(R) = E_t(R) - \lim_{R \rightarrow \infty} E_t(R)$

FIG. 6. van der Waals minima of the lowest $^3\Sigma_u$ state for $B = 0.0, 0.2, 0.5, 1.0, 2.0$ and 100.0 *a.u.*; the energy is shown with respect to the dissociation limit i.e., $E(R) = E_t(R) - \lim_{R \rightarrow \infty} E_t(R)$

FIG. 7. Total energy of the $^1\Sigma_g$ and $^3\Sigma_u$ state for $B = 0.0$ *a.u.* (all quantities are given in atomic units)

FIG. 8. Total energy of the $^1\Sigma_g$ and $^3\Sigma_u$ state for $B = 0.5$ *a.u.* (all quantities are given in atomic units)

TABLE I. Data for the lowest $^1\Sigma_g$ state: Total E_{t1} and dissociation E_d energies at the equilibrium internuclear distance, the equilibrium internuclear distances R_{eq} , the positions R_{max} and total E_{t2} energies for the maximum and the total energies in the dissociation limit $\lim_{R \rightarrow \infty} E_t$. (all quantities are given in atomic units). Transition states appear for field strengths larger than 1.0 *a.u.*.

B	R_{eq}	E_d	E_{t1}	R_{max}	E_{t2}	$\lim_{R \rightarrow \infty} E_t$
0.0	1.40	0.173438	-1.173436	—	—	-0.999998
		0.173892	-1.173892 ^a			
0.001	1.40	0.173438	-1.173436	—	—	-0.999998
0.005	1.40	0.173440	-1.173424	—	—	-0.999984
0.01	1.40	0.173450	-1.173396	—	—	-0.999946
0.05	1.40	0.173658	-1.172407	—	—	-0.998750
0.1	1.39	0.174608	-1.169652	—	—	-0.995043
0.2	1.39	0.178001	-1.158766	—	—	-0.980756
0.5	1.33	0.194663	-1.089082	—	—	-0.894419
1.0	1.24	0.228031	-0.890336	11.70	-0.662307	-0.662305
2.0	1.09	0.291170	-0.335574	7.02	-0.044395	-0.044405
5.0	0.86	0.438015	1.801212	5.15	2.239295	2.239227
10.0	0.70	0.615473	5.889023	4.23	6.504650	6.504496
50.0	0.417	1.371618	42.592815	2.86	43.964915	43.964433
100.0	0.334	1.913452	90.506974	2.48	92.421063	92.420426

^alarger basis set (see text)

TABLE II. Comparison of the total energies E_t as well as equilibrium internuclear distances R_{eq} for the lowest $^1\Sigma_g$ state with existing results in the literature in the presence of a magnetic field (all quantities are given in atomic units except for the last column which is in per cent)

B	Ref. [27]		Ref. [28] ^a		Present work		Δ_E [%] ^b
	R_{eq}	E_t	R_{eq}	E_t	R_{eq}	E_t	
0.4254414	1.337	-1.0822			1.349	-1.110362	2.60
0.5			1.29	1.06	1.33	-1.089082	2.74
1.0			1.17	0.83	1.24	-0.890336	7.27
2.127207	1.203	-0.1811			1.070	-0.255591	41.13
4.254414	0.859	1.3326			0.898	1.233808	7.41
21.27207	0.528	16.0595			0.550	15.849134	1.33
42.54414	0.463	35.76			0.440	35.558125	0.57

^aEnergy and equilibrium distance may vary to some extent since only PECs and no numerical data are given in Ref. [28].

^b Δ is the improvement in the total energy of our results on the existing data of Refs. [27, 28], respectively.

TABLE III. Data for the lowest $^1\Sigma_u$ state: Total E_t and dissociation E_d energies at the equilibrium internuclear distance, the equilibrium internuclear distances R_{eq} and total energies in the dissociation limit $\lim_{R \rightarrow \infty} E_t$ (all quantities are given in atomic units)

B	R_{eq}	E_d	E_t	$\lim_{R \rightarrow \infty} E_t$
0.0	2.42	0.131112	-0.756111	-0.624999
0.001	2.42	0.131112	-0.756109	-0.624997
0.005	2.42	0.131140	-0.756097	-0.624957
0.01	2.42	0.131246	-0.756069	-0.624823
0.05	2.43	0.132568	-0.753408	-0.620839
0.1	2.46	0.136370	-0.746347	-0.609977
0.2	2.53	0.147250	-0.722812	-0.575562
0.5	2.50	0.180626	-0.602596	-0.421969
1.0	2.30	0.225593	-0.316748	-0.091155
2.0	2.01	0.291037	0.389051	0.680087
5.0	1.60	0.414834	2.857162	3.271996
10.0	1.30	0.542594	7.327008	7.869602
50.0	0.666	0.837018	45.524983	46.362001
100.0	0.490	1.046760	94.391271	95.438032

TABLE IV. Total E_{t1}, E_{t2} and dissociation energies E_{d1}, E_{d2} at the equilibrium internuclear distance, equilibrium internuclear distances R_{eq1}, R_{eq2} and total energies in the dissociation limit $\lim_{R \rightarrow \infty} E_t$ for the lowest ${}^3\Sigma_g$ state (all quantities are given in atomic units)

B	R_{eq1}	E_{d1}	E_{t1}	R_{eq2}	E_{d2}	E_{t2}	$\lim_{R \rightarrow \infty} E_t$
0.0	1.87	0.112124	-0.737124	—	—	—	-0.624999
0.001	1.87	0.112104	-0.738101	—	—	—	-0.625997
0.005	1.87	0.112071	-0.742027	—	—	—	-0.629957
0.01	1.87	0.111865	-0.746688	—	—	—	-0.634823
0.05	1.86	0.108885	-0.779724	10.82	6.29×10^{-4}	-0.671469	-0.670839
0.1	1.84	0.101538	-0.811515	10.55	6.90×10^{-4}	-0.710667	-0.709977
0.2	1.82	0.085048	-0.860609	9.72	1.004×10^{-3}	-0.776566	-0.775562
0.5	1.81	0.062317	-0.984286	8.17	1.603×10^{-3}	-0.923572	-0.921969
1.0	1.76	0.065670	-1.156825	7.18	1.910×10^{-3}	-1.093065	-1.091155
2.0	1.55	0.090984	-1.410897	6.91	1.660×10^{-3}	-1.321573	-1.319913
5.0	1.20	0.168071	-1.896074	7.35	9.66×10^{-4}	-1.728970	-1.728004
10.0	0.96	0.274453	-2.404851	7.68	6.13×10^{-4}	-2.131011	-2.130398
50.0	0.560	0.781791	-4.245251	8.19	2.11×10^{-4}	-3.463671	-3.463461
100.0	0.446	1.162187	-5.415591	—	—	—	-4.253404

TABLE V. Data for the lowest ${}^3\Sigma_u$ state: Total E_t and dissociation E_d energies at the equilibrium internuclear distance, the equilibrium internuclear distances R_{eq} and total energies in the dissociation limit $\lim_{R \rightarrow \infty} E_t$ (all quantities are given in atomic units).

B	R_{eq}	E_d	E_t	$\lim_{R \rightarrow \infty} E_t$
0.0	7.9	1.885×10^{-5}	-1.0000173	0.9999985
0.001	7.9	1.897×10^{-5}	-1.0010170	-1.0009981
0.005	7.9	1.913×10^{-5}	-1.0050030	-1.0049839
0.01	7.9	1.919×10^{-5}	-1.0099656	-1.0099464
0.05	7.9	1.917×10^{-5}	-1.0487690	-1.0487499
0.1	7.8	1.935×10^{-5}	-1.0950628	-1.0950434
0.2	7.7	2.060×10^{-5}	-1.1807764	-1.1807558
0.5	7.4	1.532×10^{-5}	-1.3944338	-1.3944185
1.0	7.5	0.373×10^{-5}	-1.6623090	-1.6623053
2.0	—	—	—	-2.0444046
5.0	—	—	—	-2.7607732
10.0	—	—	—	-3.4955044
50.0	—	—	—	-6.0355668
100.0	—	—	—	-7.5795742

Fig. 1

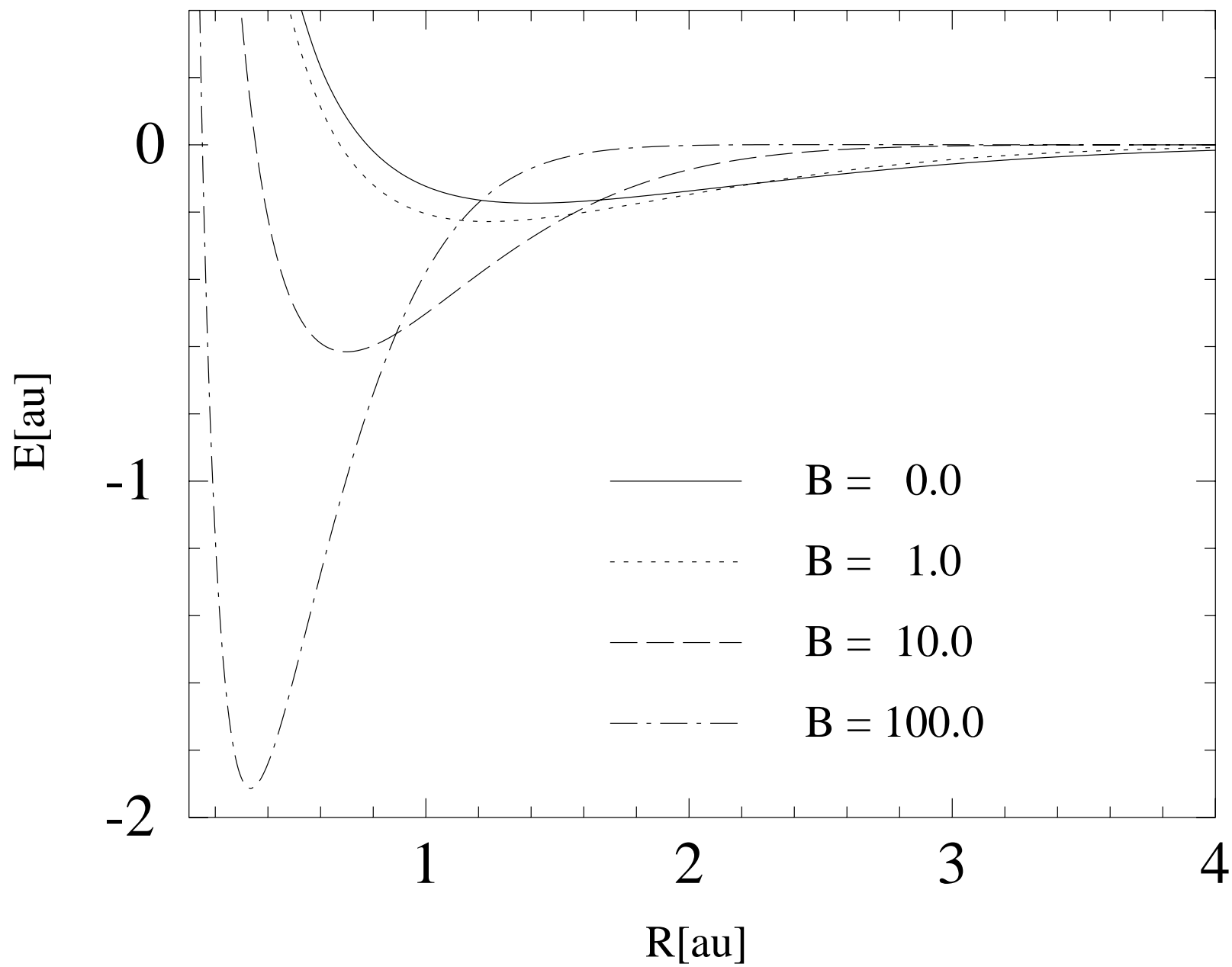


Fig. 2

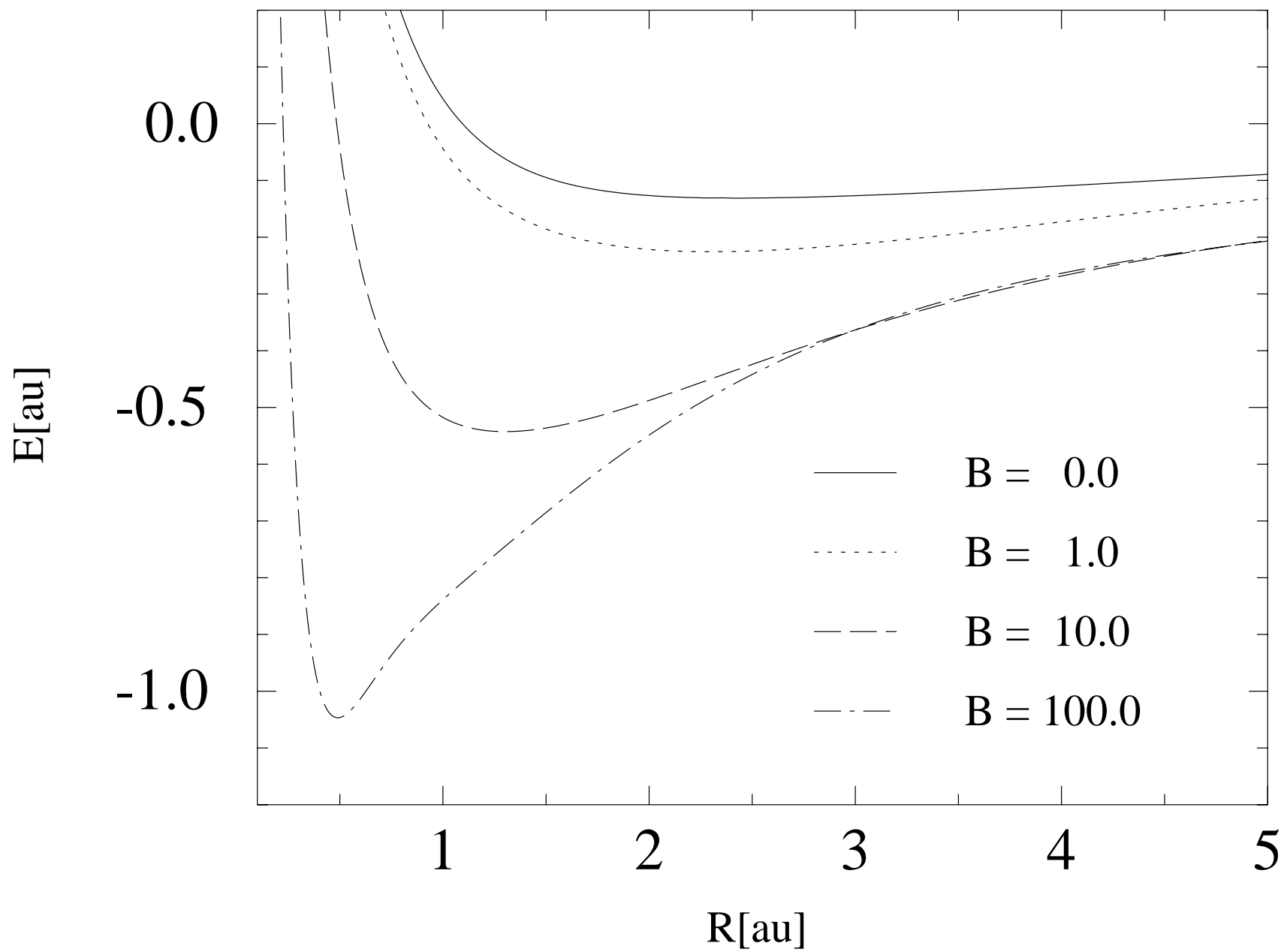


Fig. 3

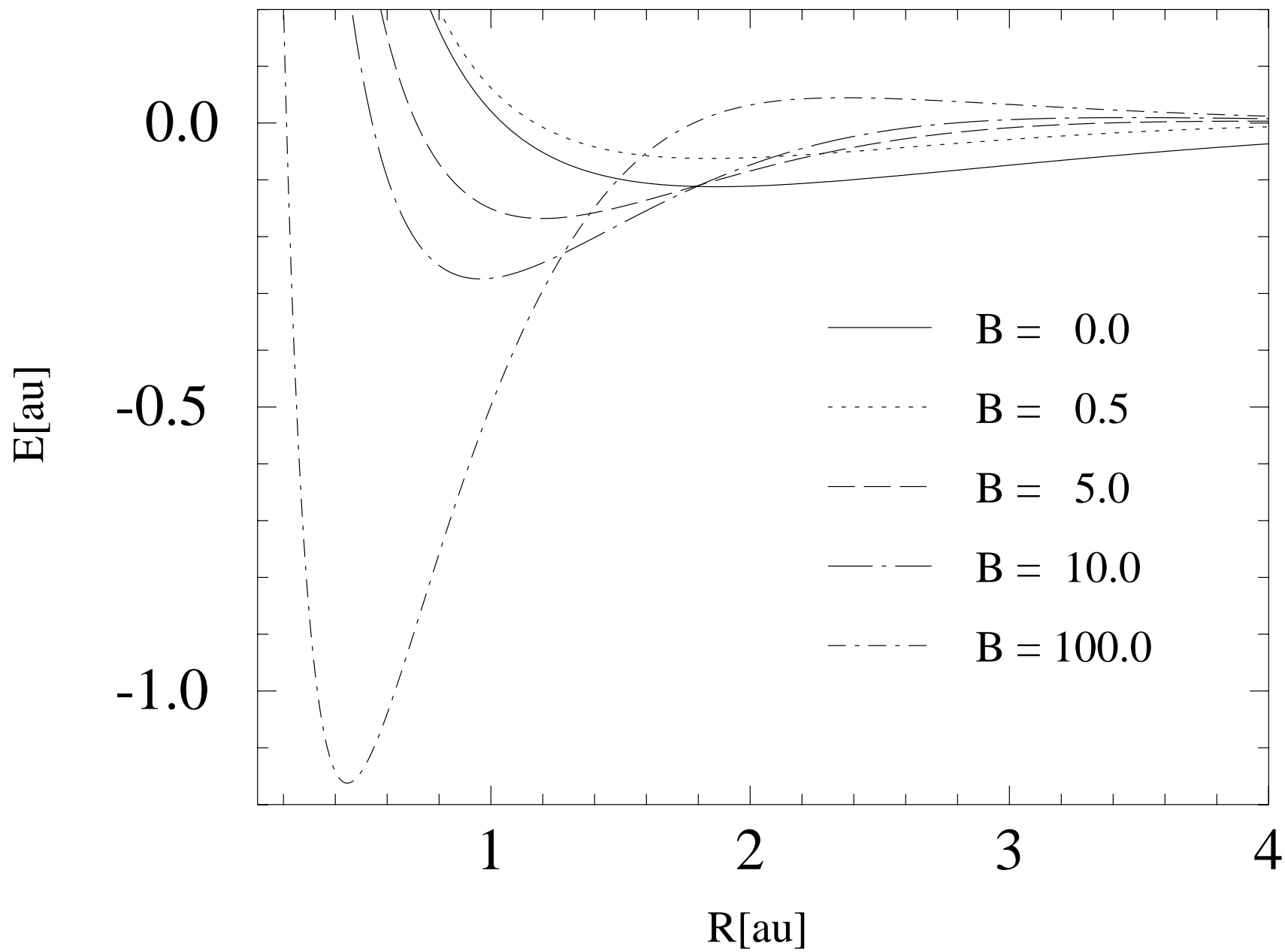


Fig. 4

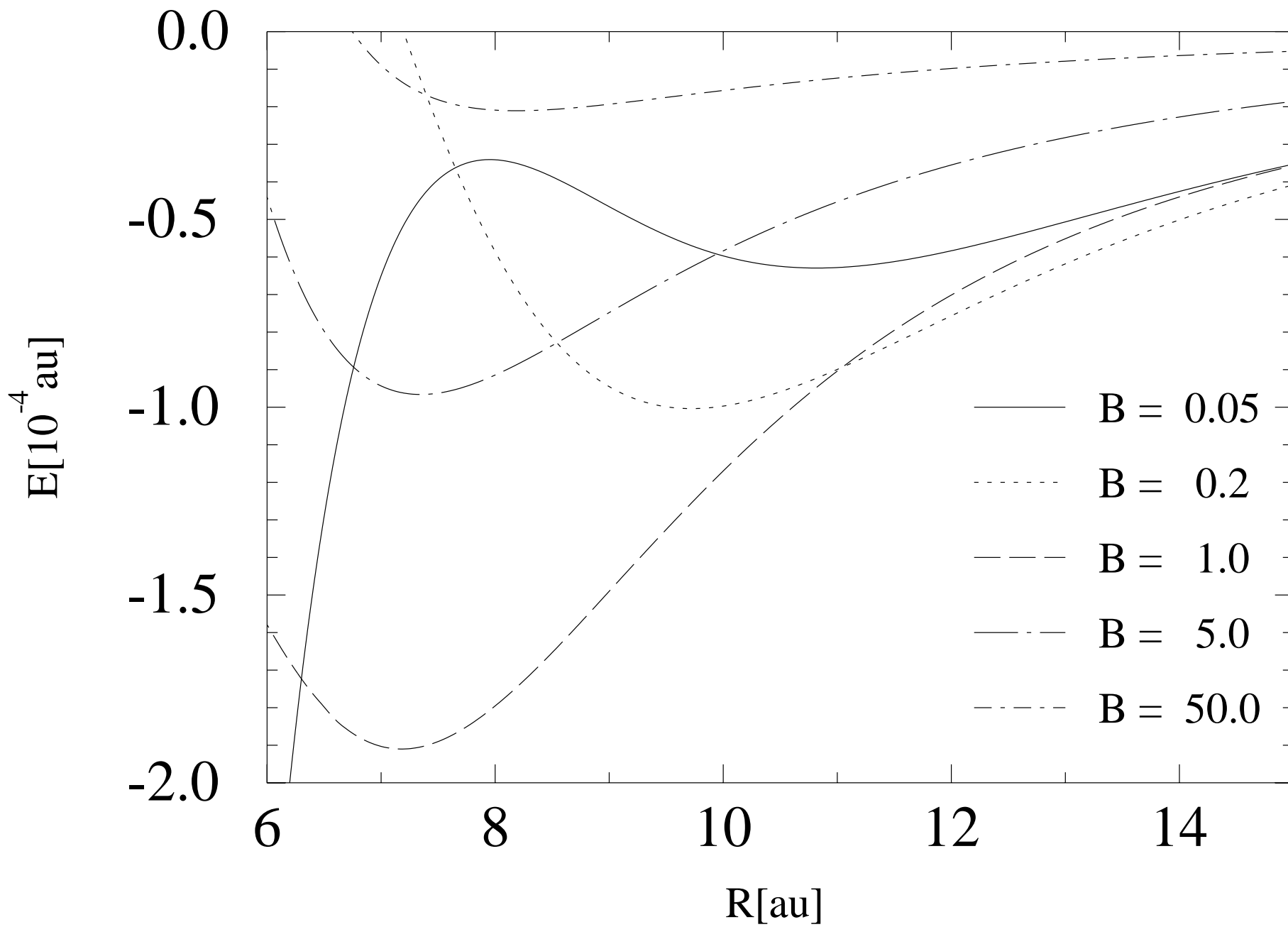


Fig. 5

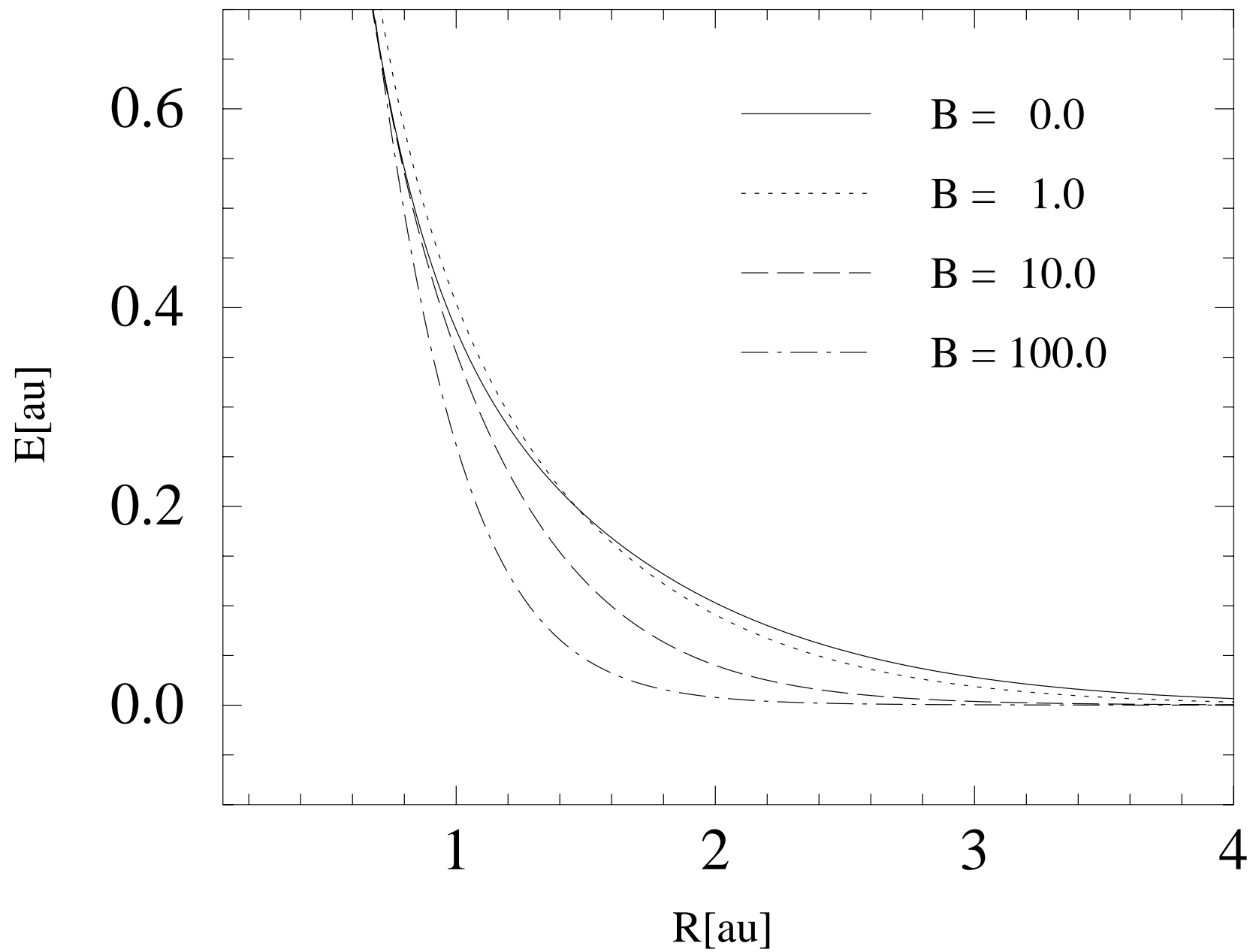


Fig. 6

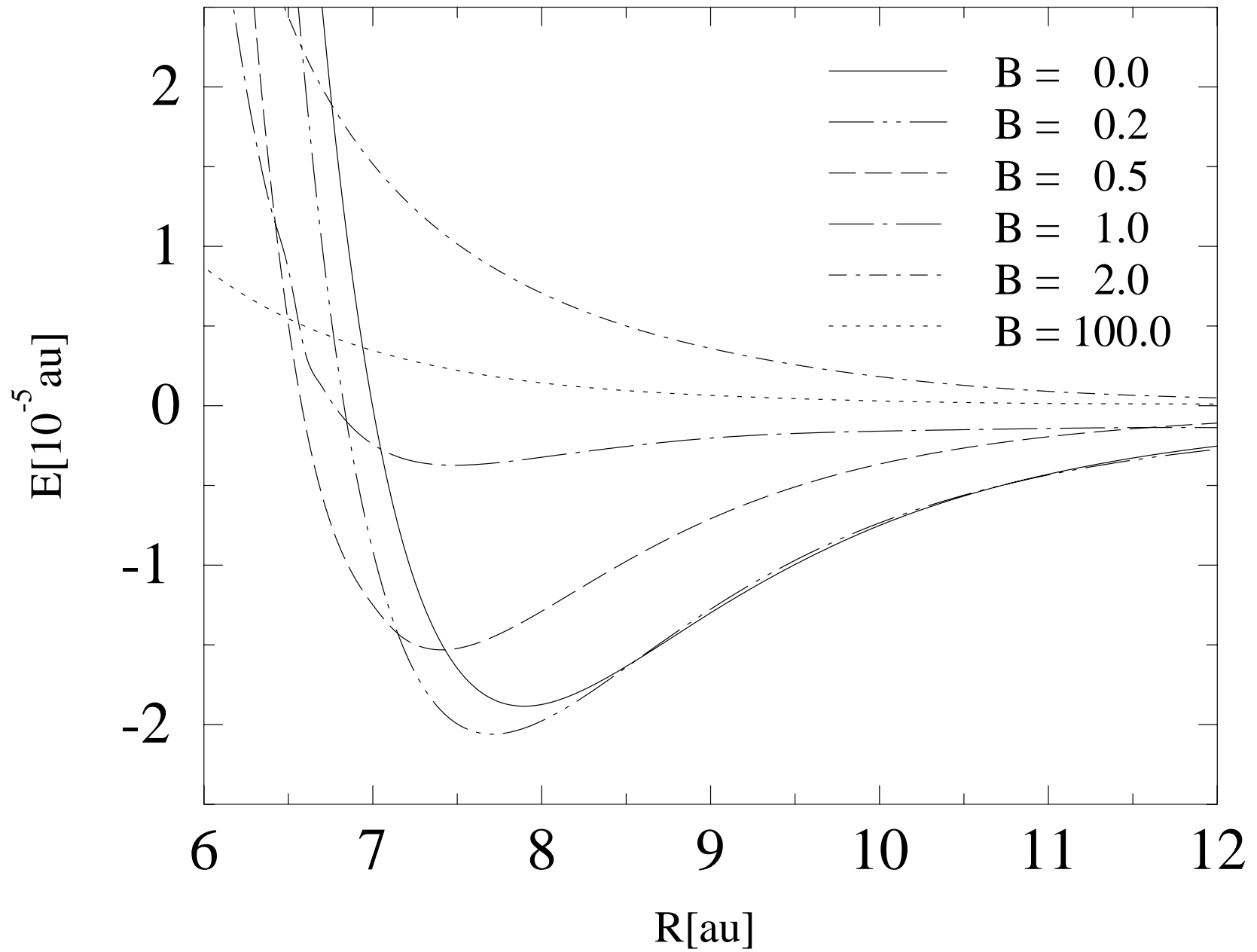


Fig. 7

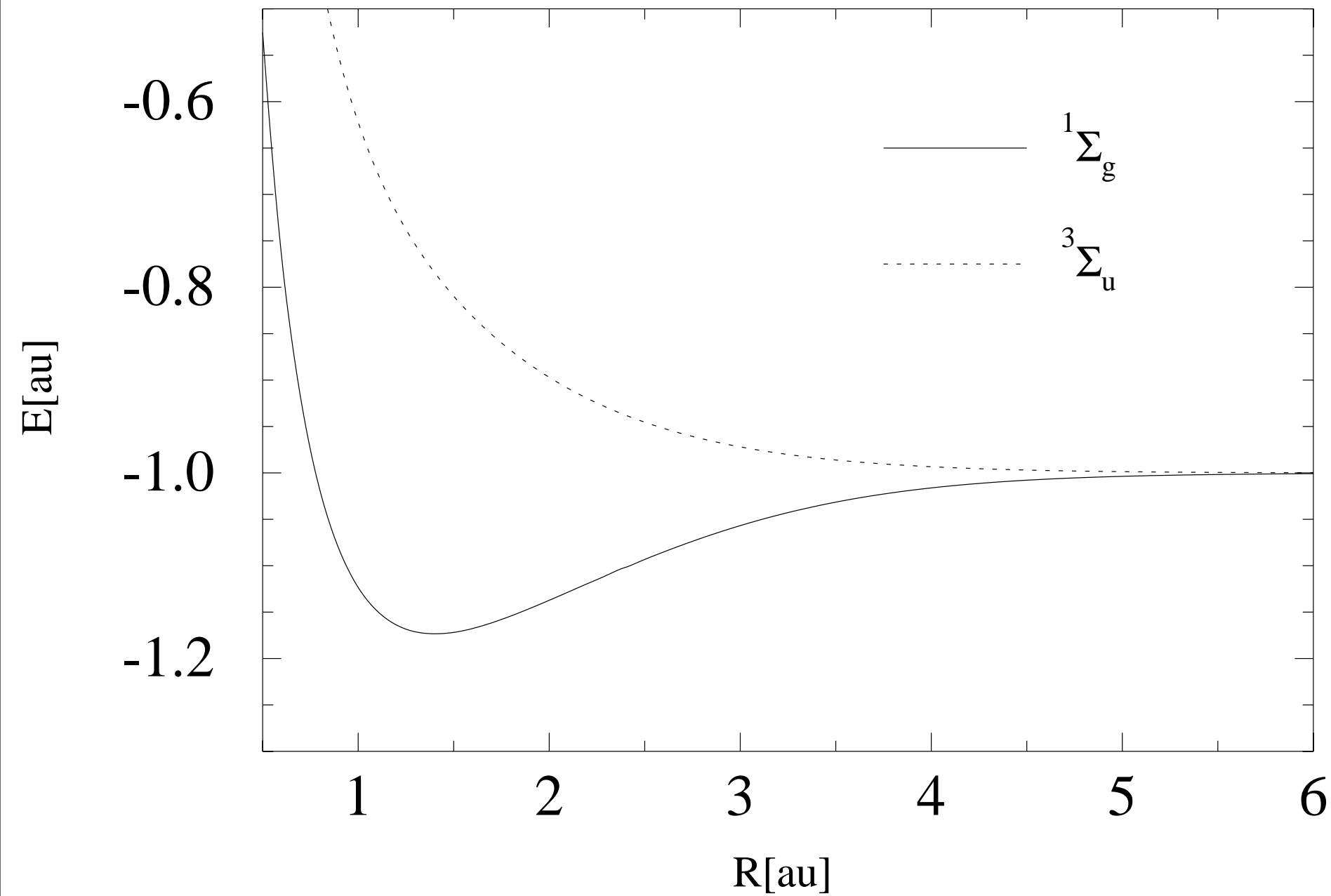


Fig. 8

